Supplementary

Structural features and antiproliferative activity of Pd(II) complexes with halogenated ligands: A comparative study between Schiff base and reduced Schiff base complexes

Kimia Forooghi[a], Hadi Amiri Rudbari[a,*], Claudio Stagno[b], Nunzio Iraci[b], José V. Cuevas-Vicario[c], Nazanin Kordestani[d], Tanja Schirmeister[e], Thomas Efferth[f], Ejlal A. Omer[f], Nakisa Moini[g], Mahnaz Aryaeifar[a], Olivier Blacque[h], Reza Azadbakht[i], Nicola Micale[b,*]

[a] *Department of Chemistry, University of Isfahan, Isfahan 81746-73441, Iran.*

[b] *Department of Chemical, Biological, Pharmaceutical and Environmental Sciences, University of Messina, Viale Ferdinando Stagno D'Alcontres 31, I-98166 Messina, Italy.*

[c] *Departamento de Química, Facultad de Ciencias, Universidad de Burgos, Plaza Misael Bañuelos s/n, 09001, Burgos, Spain.*

[d] *Área de Química Inorgánica-CIESOL Facultad de Ciencias, Universidad de Almería, Carr. Sacramento, s/n, 04120 La Cañada, Almería, Spain.*

[e] *Department of Medicinal Chemistry, Institute of Pharmaceutical and Biomedical Sciences, Johannes Gutenberg University, staudinger Weg 5, 55128 mainz, Germany.*

[f] *Department of Pharmaceutical Biology, Institute of Pharmaceutical and Biomedical Sciences, Johannes Gutenberg University, staudinger Weg 5, 55128 mainz, Germany.*

[g] *Department of Chemistry, Faculty of Physics and Chemistry Alzahra University, P.O. Box 1993891176, Vanak Tehran, Iran.*

[h] *Department of Chemistry, University of Zurich, Winterthurerstrasse 190, CH-8057, Zurich, Switzerland.*

[i] *Department of Inorganic Chemistry, Faculty of Chemistry, Bu-Ali Sina University, 6517838683, Hamedan, Iran.*

***** Corresponding authors.

E-mail addresses: h.a.rudbari@sci.ui.ac.ir, hamiri1358@gmail.com (H. Amiri Rudbari), nmicale@unime.it (N. Micale).

IR Spectra

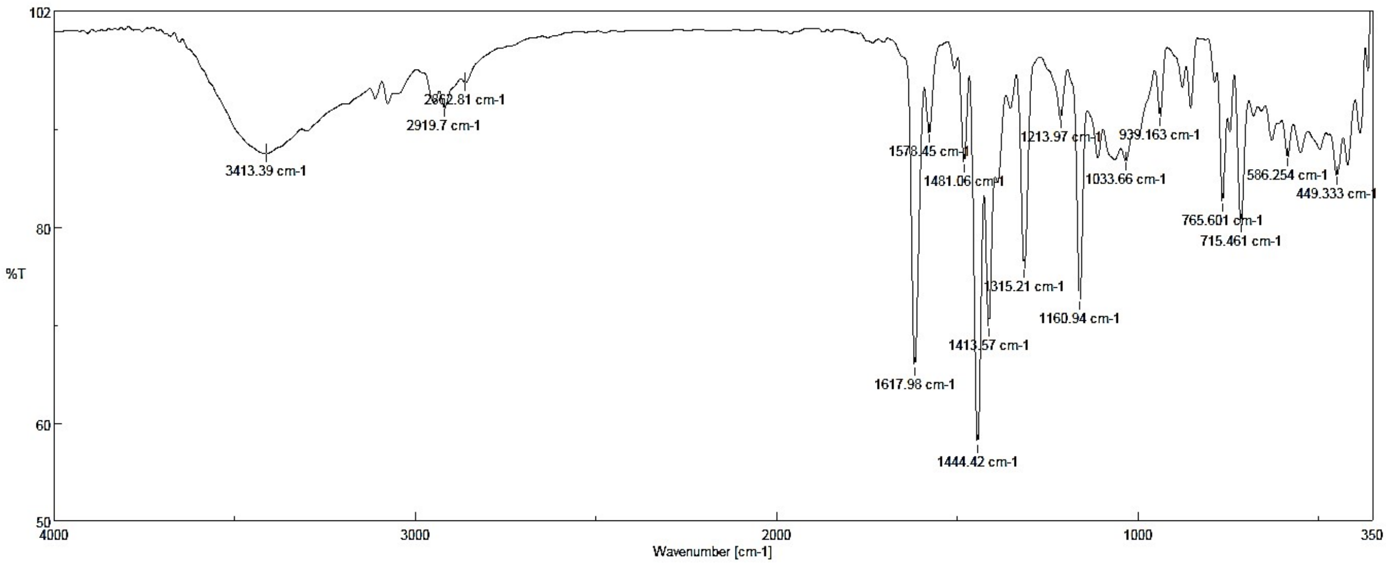

1. **Cl_2PyPd**

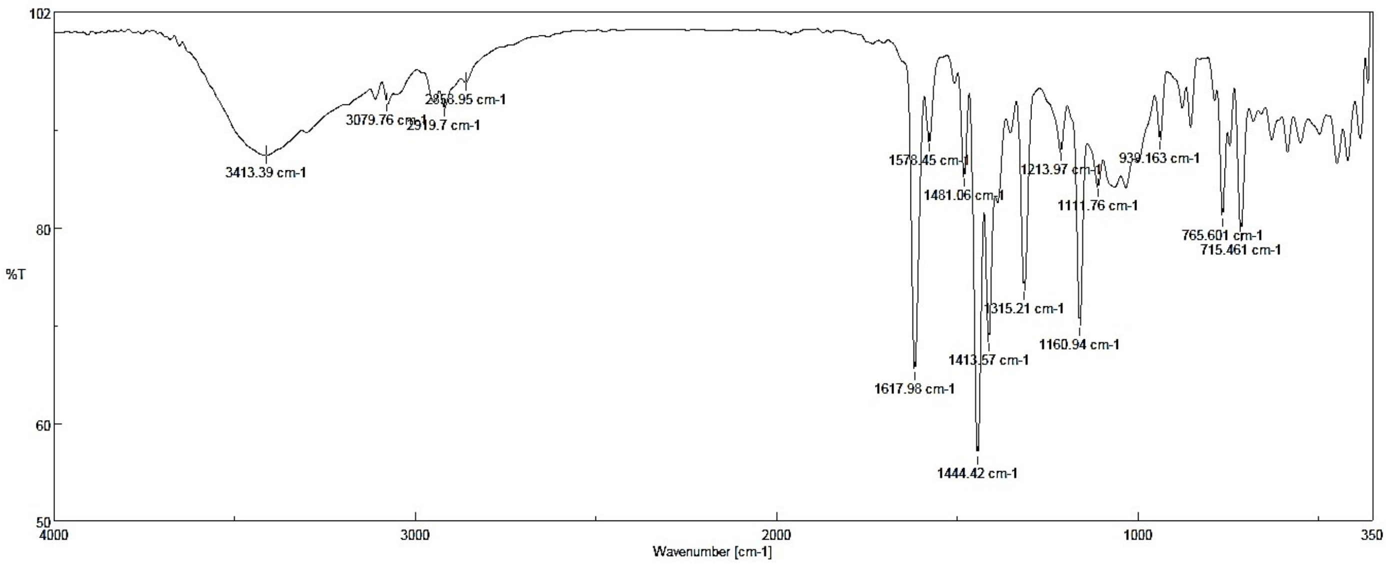

2. **Br_2PyPd**

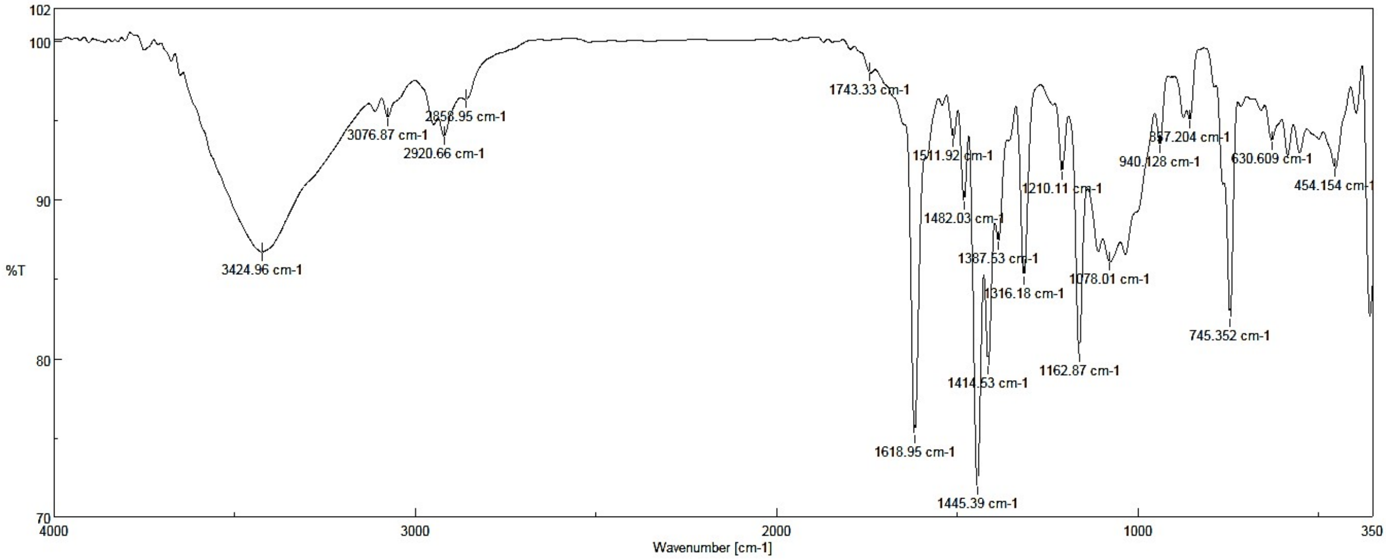

3. **ClBrPyPd**

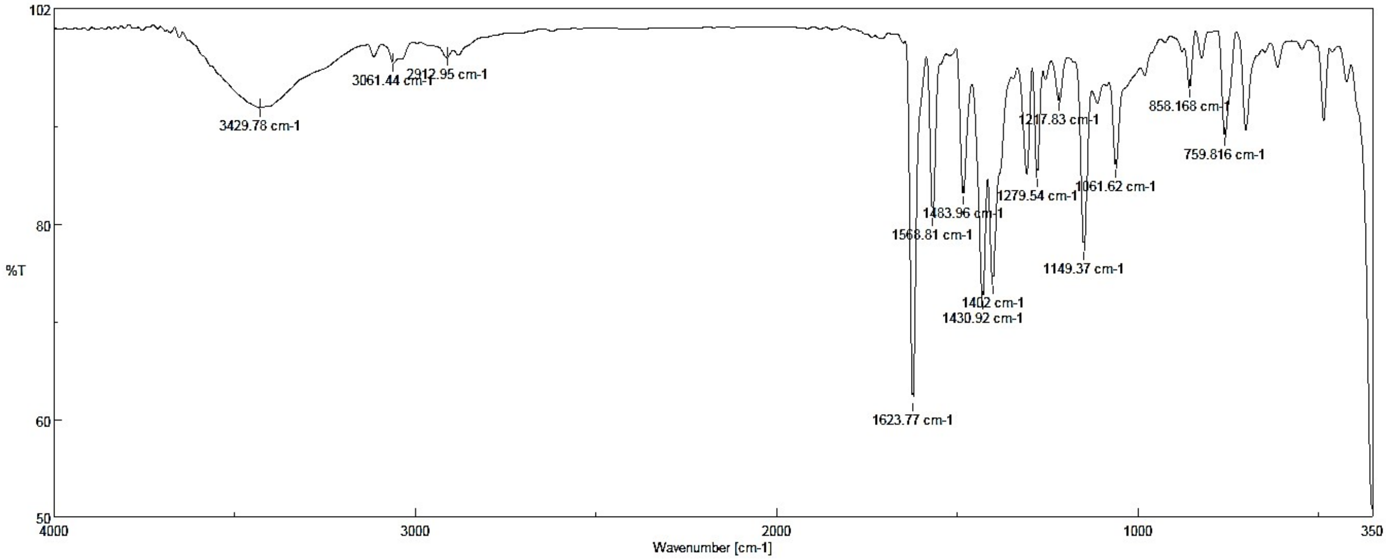

4. **I_2PicPd**

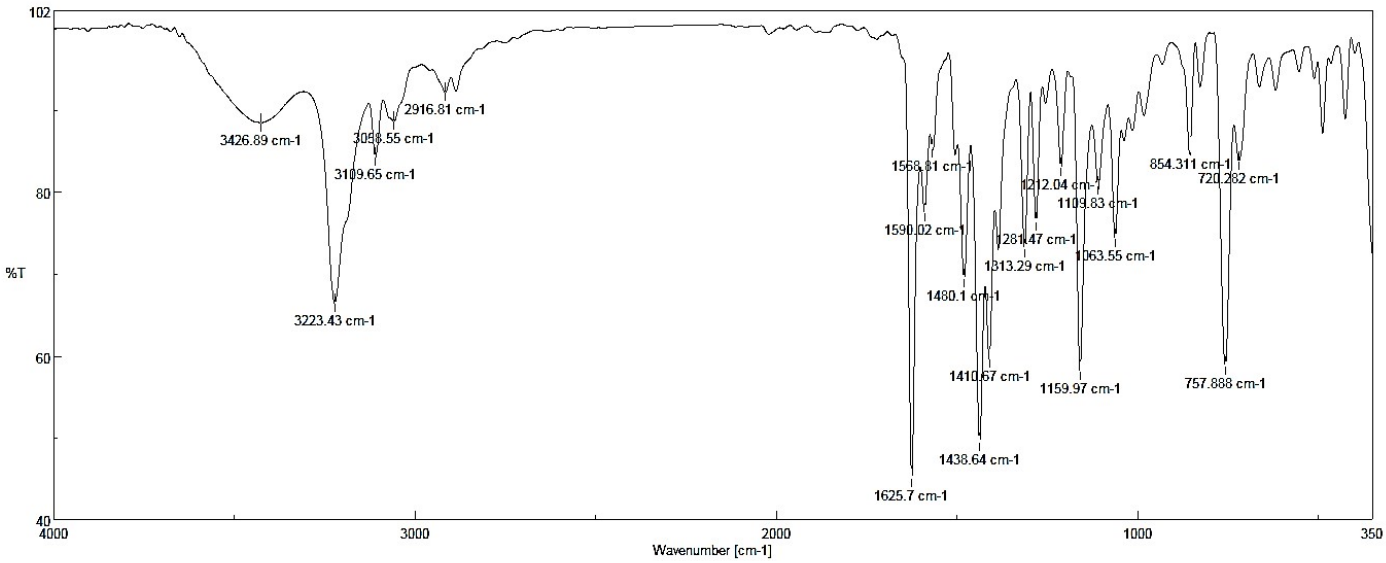

5. **ClBrPicPd**

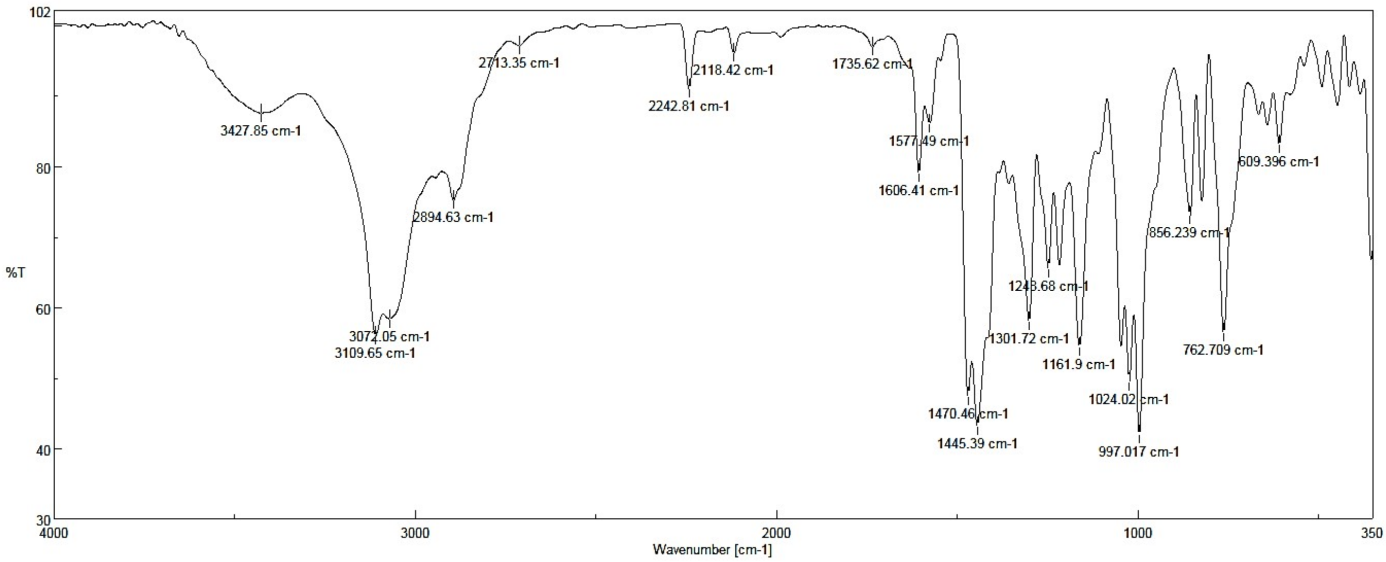

6. **Cl_2Py(R)Pd**

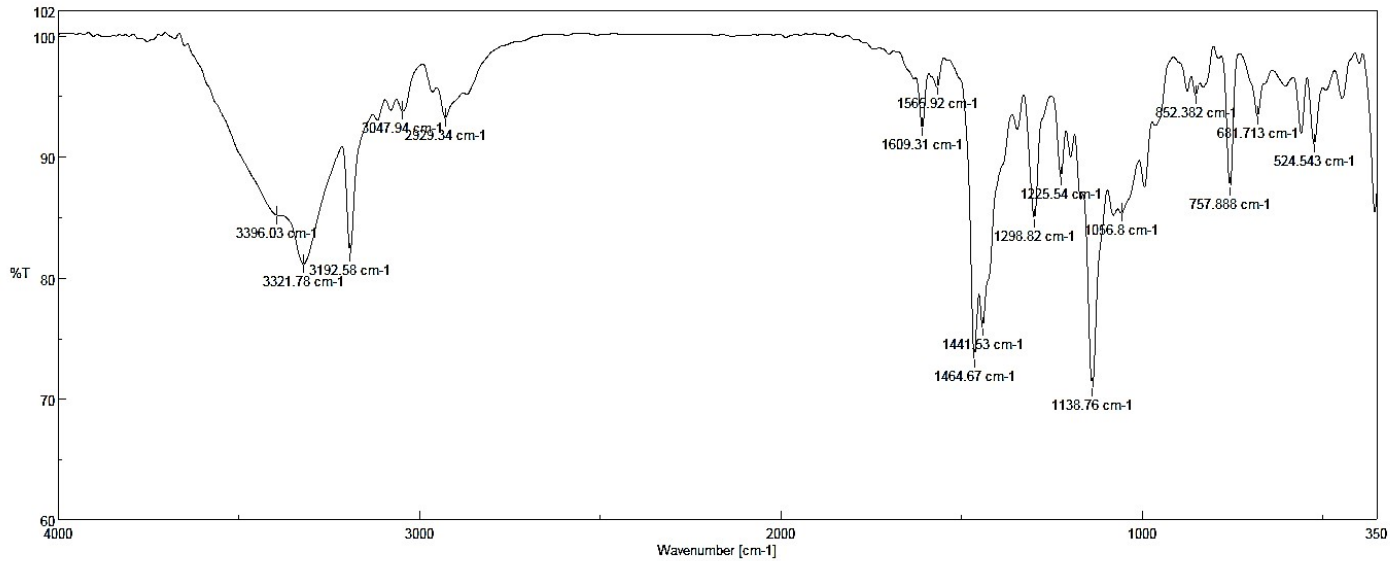

7. **$Br_2Py(R)Pd$**

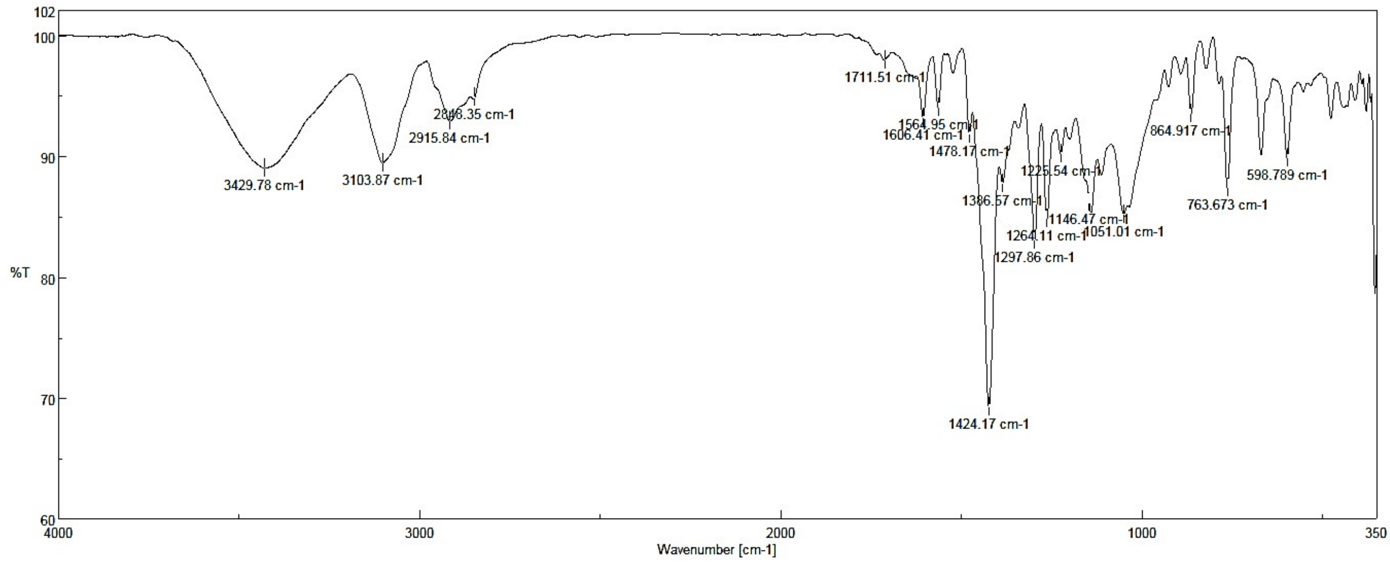

8. **$I_2Py(R)Pd$**

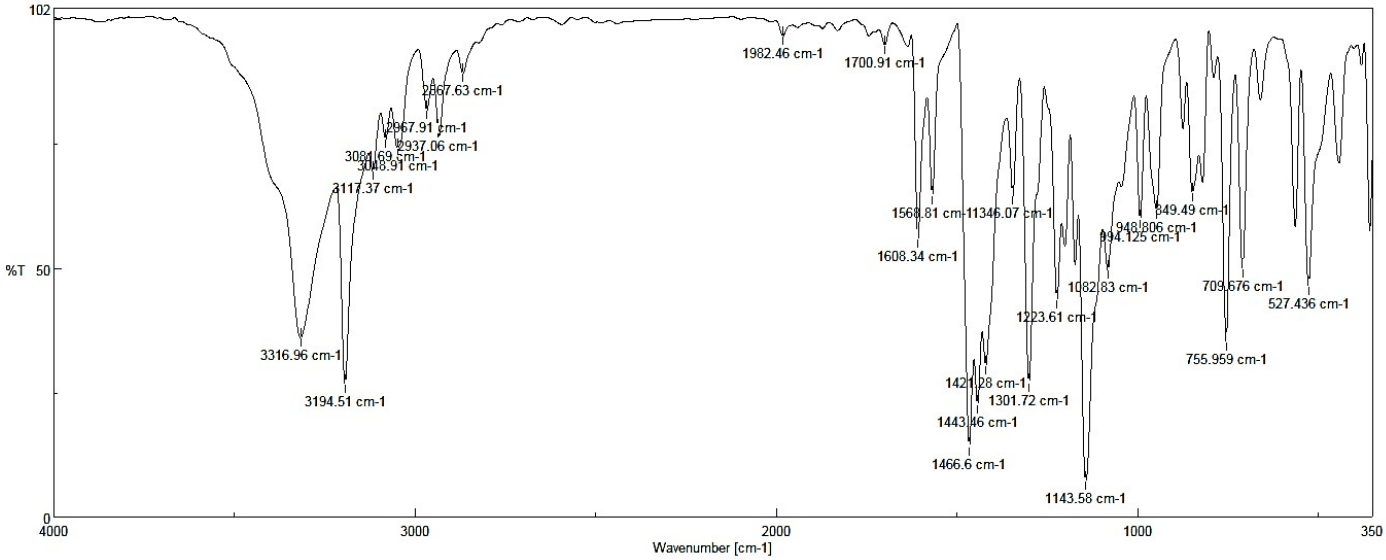

9. **ClBrPy(R)Pd**

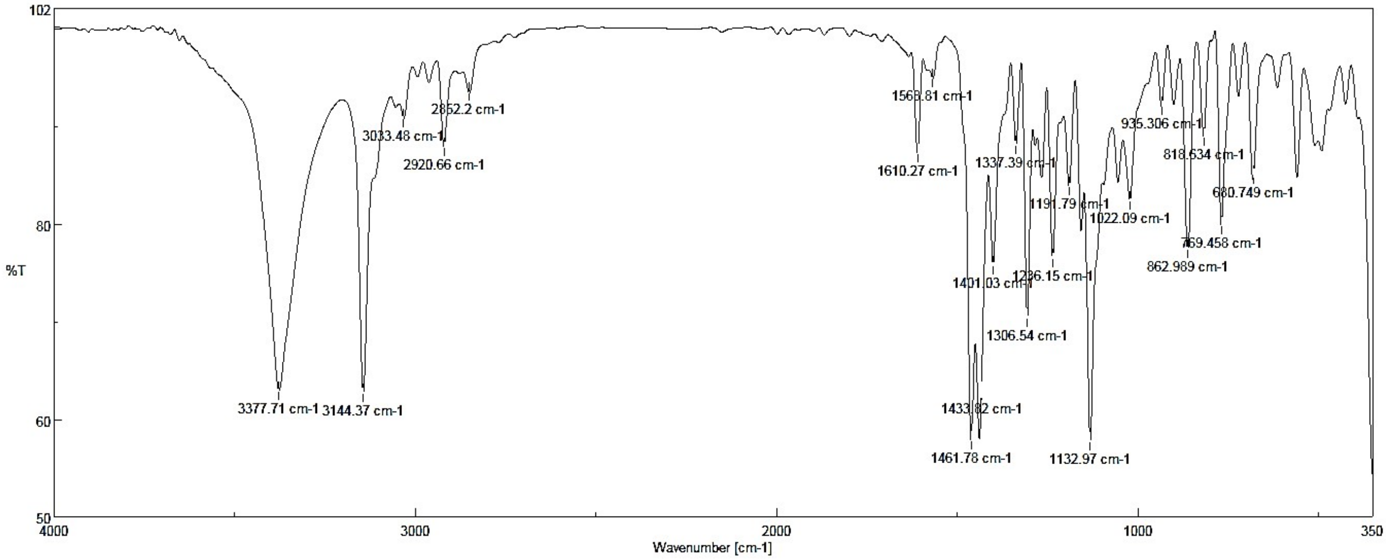

10. **Br_2Pic(R)Pd**

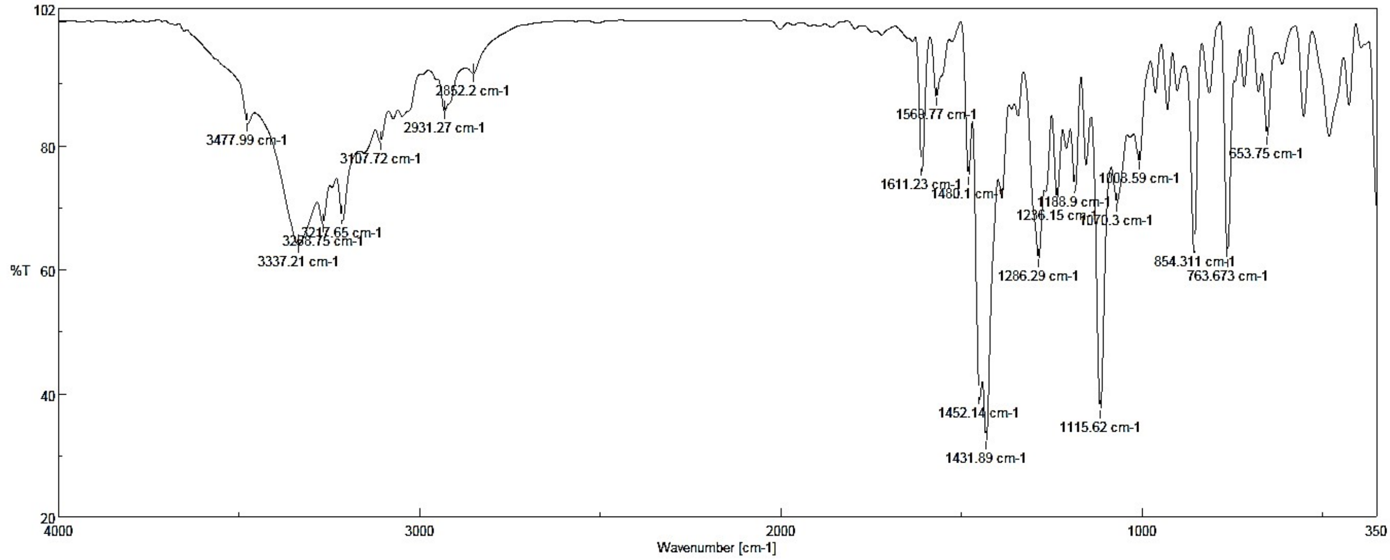

11. $\mathbf{I_2Pic(R)Pd}$

Fig. S1 IR spectra of Pd complexes (1-11).

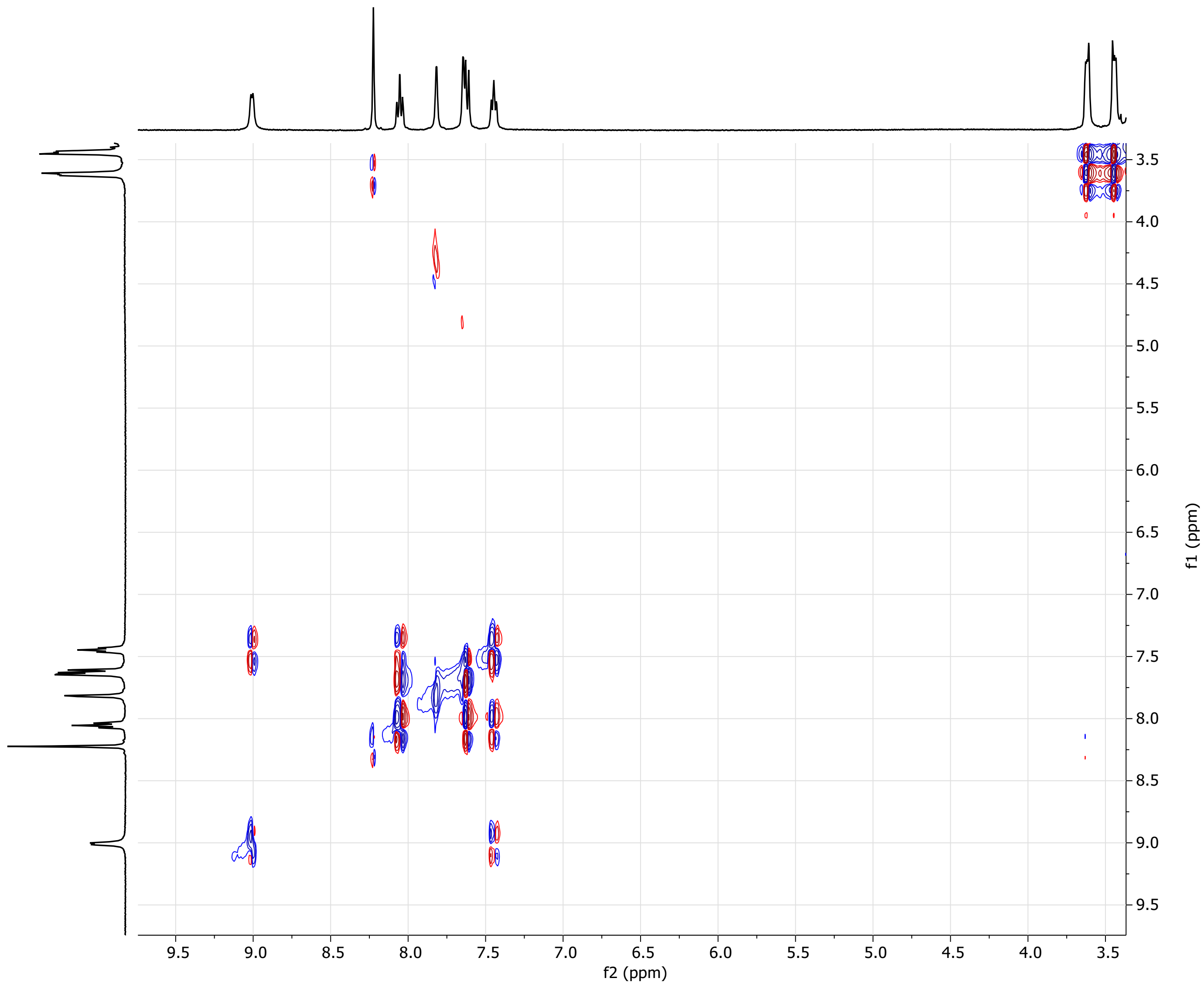

(a)

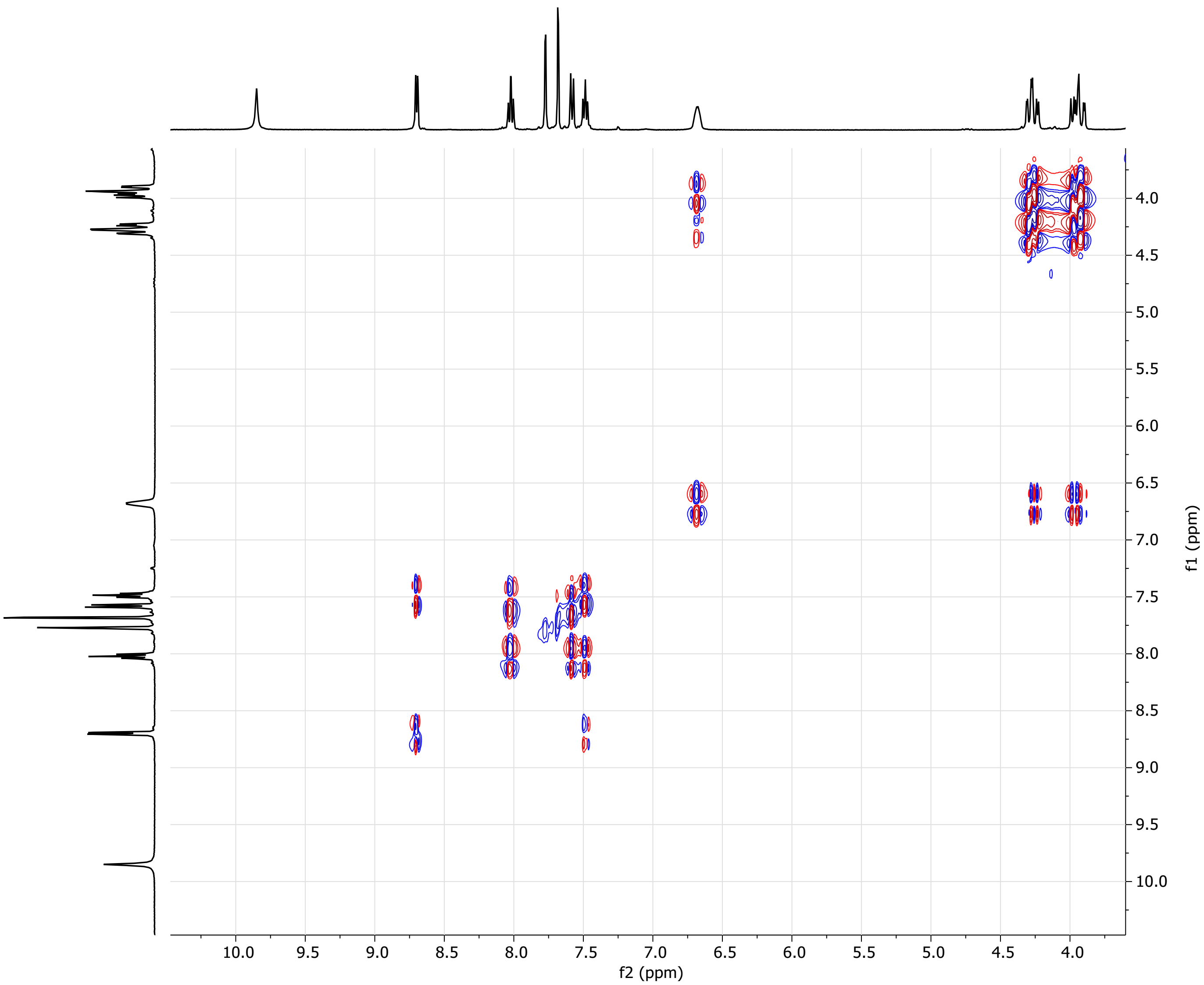

(b)

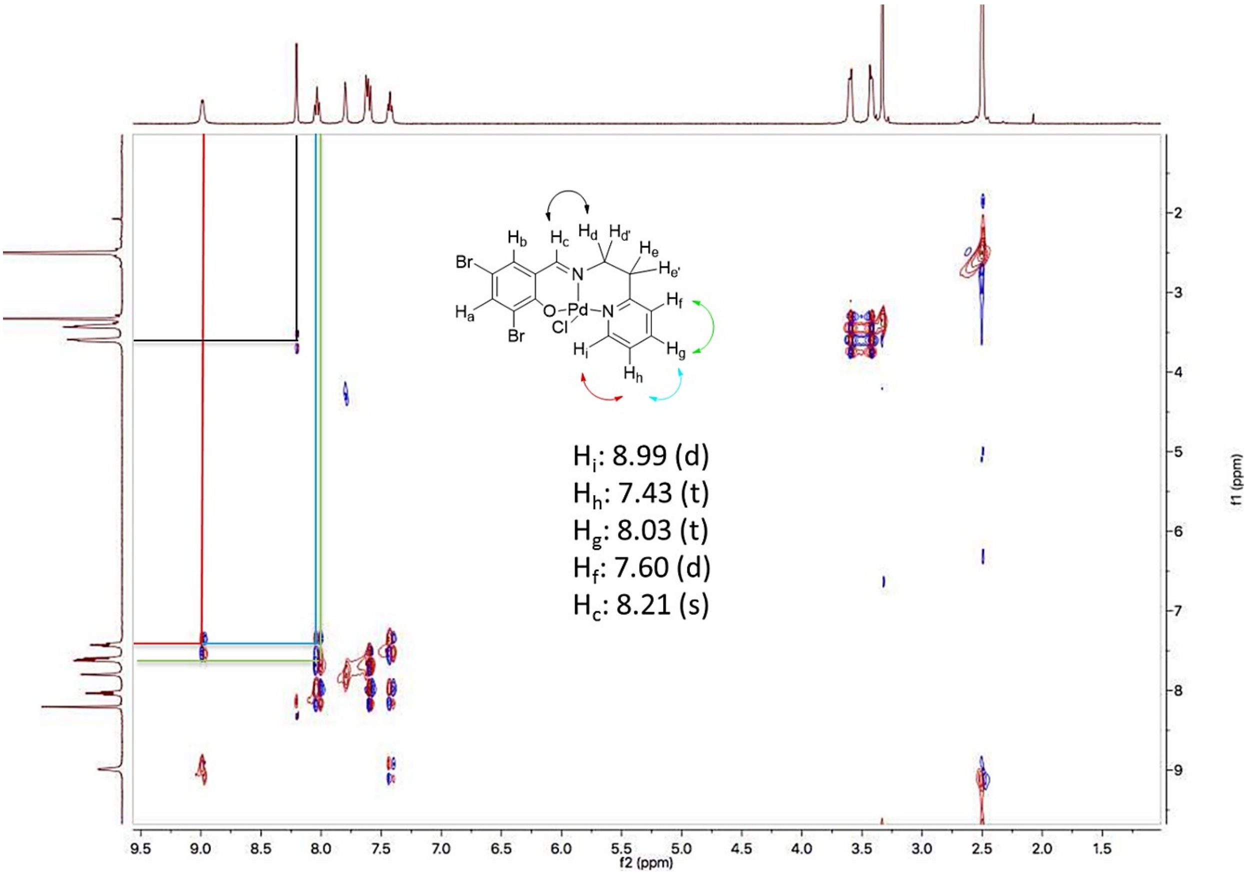

(c)

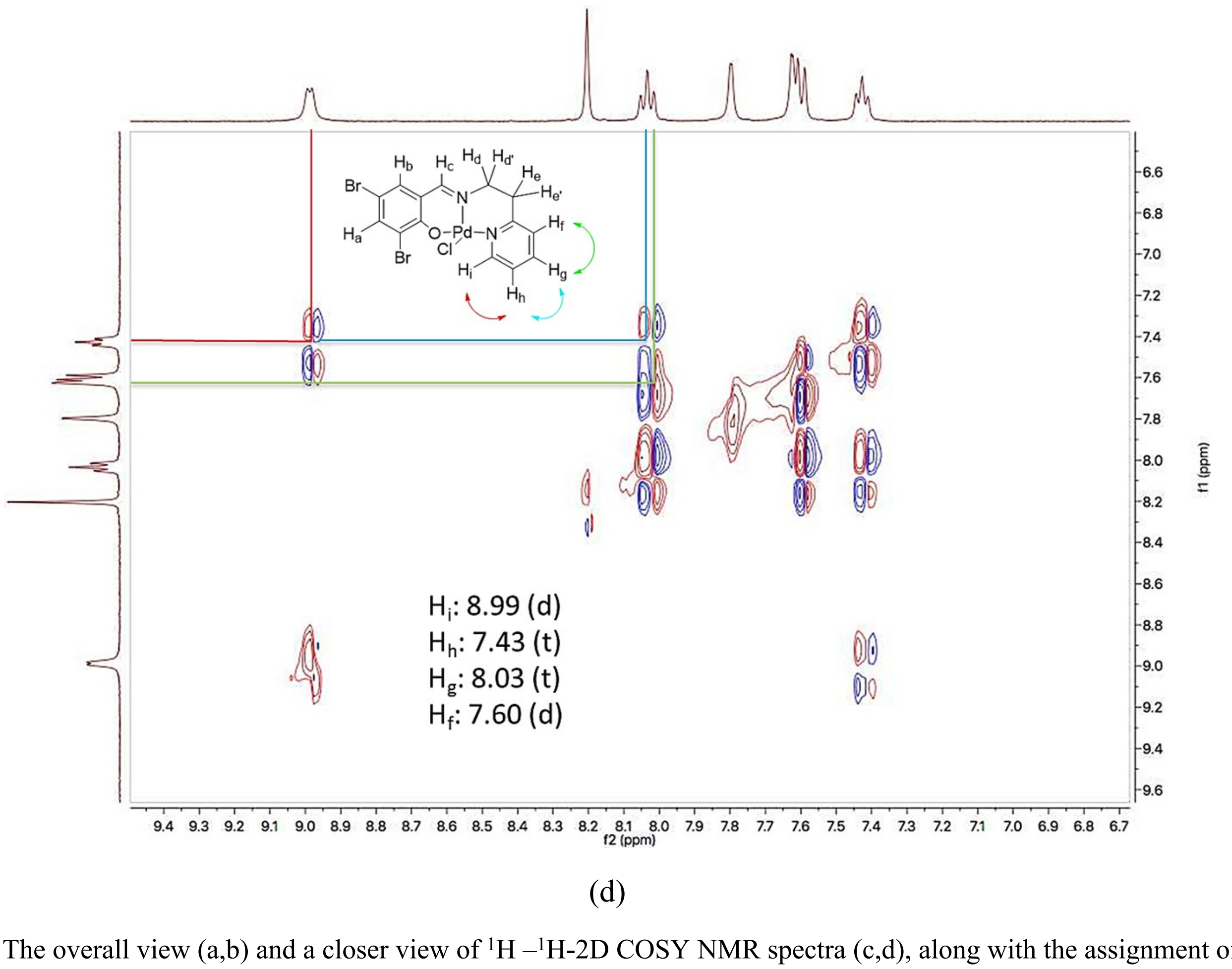

(d)

Fig. S2 The overall view (a,b) and a closer view of ^{1}H –^{1}H-2D COSY NMR spectra (c,d), along with the assignment of hydrogens in aromatic region for complex **Br$_2$PyPd**; (a,c,d: **Br$_2$PyPd**, b: **Br$_2$Pic(R)Pd**,).

Intra- and Intermolecular Interactions in crystal structure of Br_2PyPd

In the solid state structure, each **Br_2PyPd** molecule is aligned so that it is in close contact with all the seven surrounding molecules, developing the strength of the crystal lattice. The crystal packing shows seven different H-bonds with various strength, due to the diverse contact lengths and angles that the involving atoms bear: Chlorine ligand is connected to the hydrogen atom of pyridine ring through the intramolecular C(14)-H(14)…Cl(1) hydrogen bond, making a S(5) ring (Fig. S3a).

The intermolecular C(7)-H(7)…Cl(1) and C(12)-H(12)…Br(2) hydrogen bonds connect the neighboring molecules into one-dimensional extended chains along the *ac* and *c*-axis, respectively (Fig. S3b,c). Here, the chlorine atom is actually a trifurcated accepter, accepting H-bonds from three donors; intermolecular H(14)…Cl(1) H-bond is also one of them, which makes head-to-tail dimers in crystal lattice of the complex (Fig. S3d).

Fig. S3e presents a situation where multiple intermolecular interactions link two adjacent head-to-tail fashion molecules into a one-dimension chain along the *b*-axis: **1**) an array of hydrogen bond donors and acceptors, in which O(1) is a bifurcated acceptor (C(8)-H(8B)…O(1)…H(9B)-C(9)), and C(8) is a bifurcated donor (Pd-O(1)…H(8B)…Cl(1)-Pd), making S(4) and S(6) rings, respectively; **2**) a n→π* interaction (Cl→ $_{iminic}$C(7)=N(2), 3.38 Å), where lone pair electrons of Cl ligand (n) is donated into the empty π* orbital of the nearby imine group (C=N), and leading to an attractive interaction that is shorter than the sum of the van der Waals radii of Cl and C [Σr_{vdW} = 3.45 Å]. It is noteworthy that the lone pair electrons of Cl atom are participated simultaneously as the donor of hydrogen bond (C(8)-H(8B)…Cl), and the donor of n→π* interaction; **3**) and also an CH…π interaction, ($_{aliphatic}$C(9)-H(9B)…C(1)$_{aromatic}$), where one hydrogen atom from a sp^3 carbon points towards the C1=C6 bond of the arene ring; **4**) The last one is a face-to-face π…π interaction, whereby nearly parallel rings (pyridine and arene ring), separated by ca. 3.7 Å (3.74, 3.78 Å), are offset and the center of one ring interacts with the corner of another (Fig. S3f).

Br_2PyPd

Intramolecular Interactions

a
H-bonding
(C14H14…Cl1)

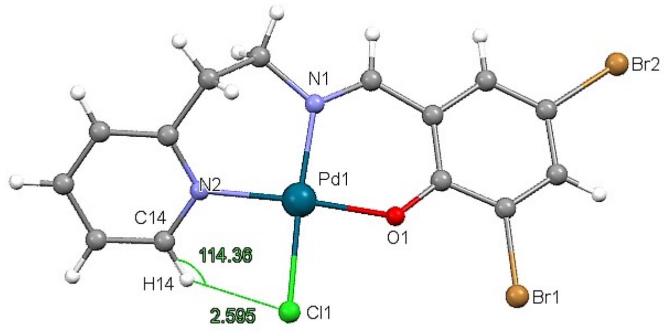

Intermolecular Interactions

b
H-bonding
(C7H7…Cl1)

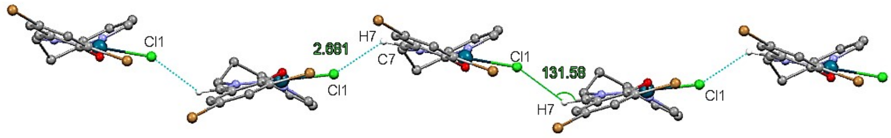

c
H-bonding
(C12H12…Br2)

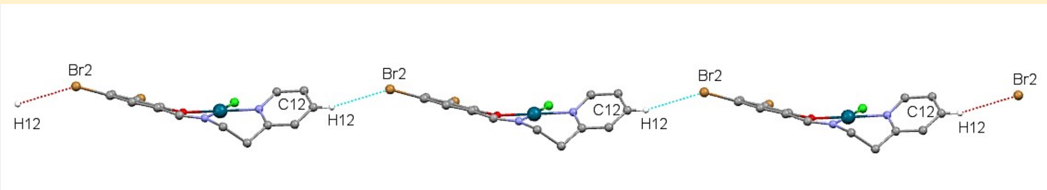

d
H-bonding
(C14H14…Cl1)

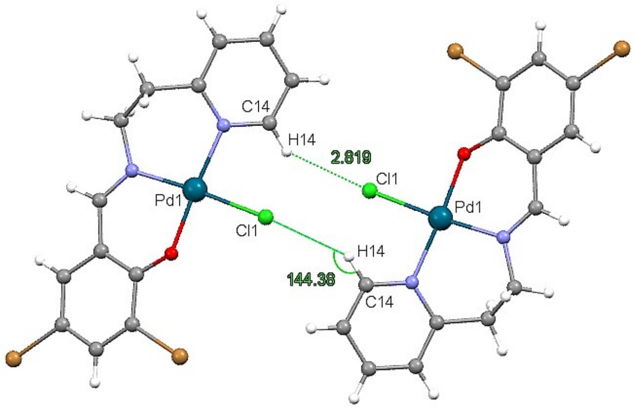

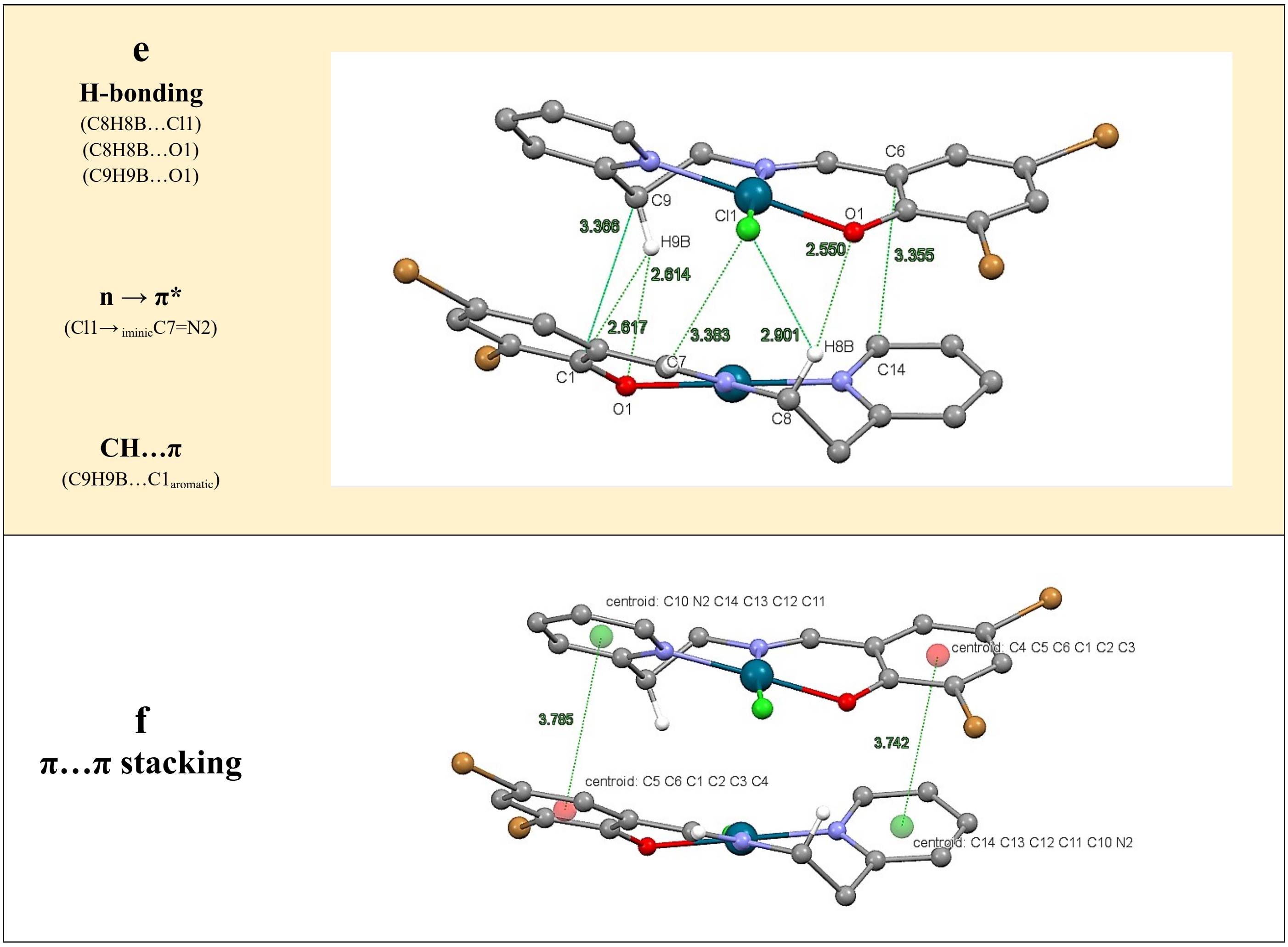

Fig. S3 Parts of the crystal packing of **Br_2PyPd**, showing different aggregation patterns made by various intra- and intermolecular interactions. Intra- (a) and intermolecular hydrogen bonds (b-e), and also mutual n → π*, CH…π (e) and π…π stacking interactions (f) between **Br_2PyPd** dimers are shown.

Intra- and Intermolecular Interactions in crystal structure of Cl_2Py(R)Pd

The distance of N(2)-C(8), [1.4888(19) and 1.491(2) Å for **Cl_2Py(R)Pd** and **ClBrPy(R)Pd** respectively], confirm the single-bond character of this bonding, which enables the molecule to rotate over this bond and adopt the most stable conformation in the solid state, that contains two intramolecular CH…π interactions, prompting the arene ring to point directly toward the hydrogen atoms of C(7) and creating a S(4) ring [$_{aliphatic}$C(7)-H_2…C(9)$_{aromatic}$] (Fig. S 4, Fig. S 5 a).

In their lattice structures, each molecule is aligned somehow that it is in close contact with all the ten surrounding molecules, increasing the strength of the solid state structure. The two Cl ligands interacted with nearby aliphatic and aromatic hydrogens in a way that made a butterfly shape of the involving atoms with the Pd atom at the center. These two interactions, together with two other intramolecular H-bonding, could somehow lock the molecules and lead to a fixed position of the corresponding atoms within the intramolecular space of the complex (Fig. S 4, Fig. S 5 b).

Fig. S 4 c, e and f represent three non-linear intermolecular hydrogen bonds [H(1)…Cl(3), H(4)…Cl(1) and H(6A)…Cl(4)], which connect the **Cl_2Py(R)Pd** molecules along *c*, *a* and *b*-axis, forming a three-dimensional network. Also Fig. S 4 d and g, show several intermolecular hydrogen bondings whereby two neighboring head-to-tail molecules are connecting through them, forming individual dimers and leading to a zero-dimensional aggregation in the lattice structure of **Cl_2Py(R)Pd**.

As for the **ClBrPy(R)Pd** complex, other than those described (above), the packing of the crystal shows several intermolecular interactions, including: **I**) halogen bonds which link the bromine substitution of the arene ring and one of the Cl ligands of the adjacent molecule, with a Cl…Br distance of 3.509 Å, that is shorter than the sum of the conventional vdW radii [Σr_{vdW} = 3.60 Å], and together with H(1)…Br H-bonds, lead to an infinite one-dimensional aggregation along the *bc*-axis (Fig. S 5 e); **II**) a number of C-H…π short contacts ($_{aliphatic}$H(8B)…C(12)$_{aromatic}$) that occur between aliphatic CH groups and π-clouds of the arene rings, joining two adjacent molecules to form head-to-tail arranged dimers (Fig. S 5 g); **III**) and also π…π stacking interactions, whereby two parallel-displaced pyridine rings with a C(2)…C(2) distance of 3.393 Å, and centroid to centroid distance of 4.483 Å are in short contact (Fig. S 5 h); **IV**) moreover, as it is being shown in Fig. S 5 with more details, this structure is further interconnected by some other Moderate-strength hydrogen bonds that are formed between neutral donor or acceptor groups.

$Cl_2Py(R)Pd$

Intramolecular Interactions

a

CH…π

($_{aliphatic}$C7-H7A…C9$_{aromatic}$)
($_{aliphatic}$C7-H7B…C9$_{aromatic}$)

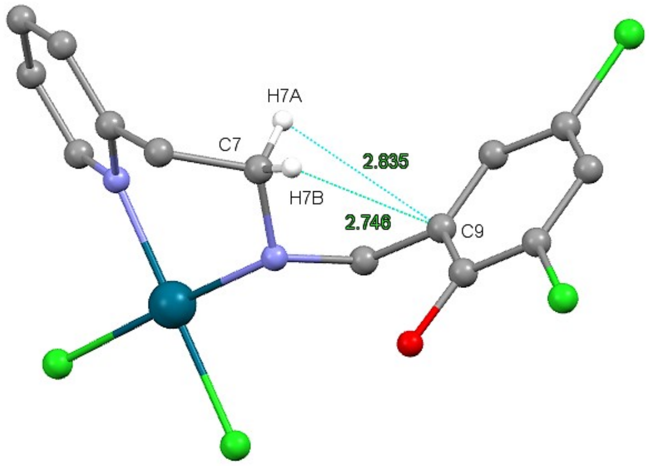

b

H-bonding

(C1H1…Cl1)
(C8H8B…Cl2)
(O1H1A…Cl3)
(N2H2A…O1)

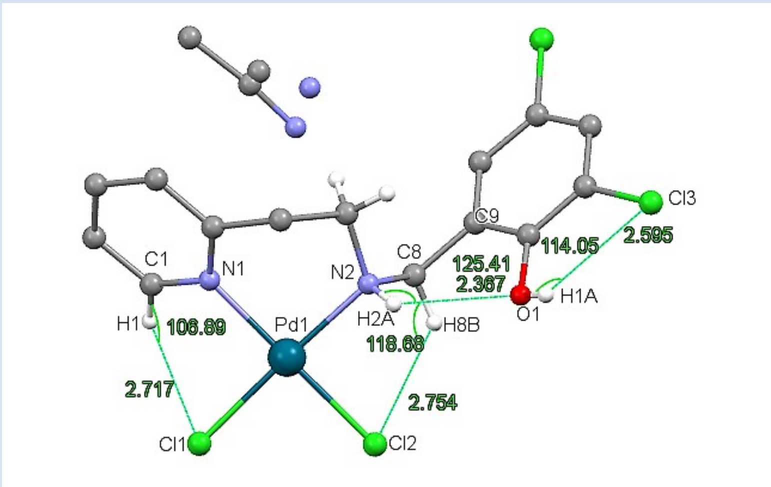

Intermolecular Interactions

c

H-bonding

(C1-H1…Cl3)

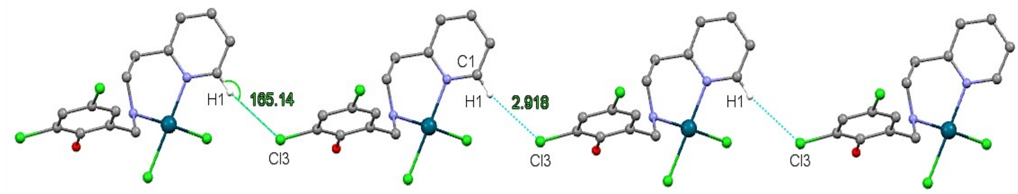

<table>
<tr><td>

d

H-bonding
(C3-H3…Cl1)

</td><td>

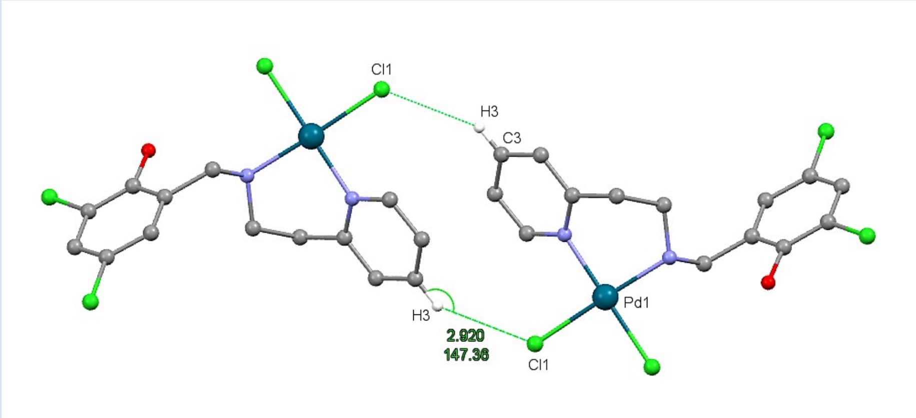

</td></tr>
<tr><td>

e

H-bonding
(C4-H4…Cl1)

</td><td>

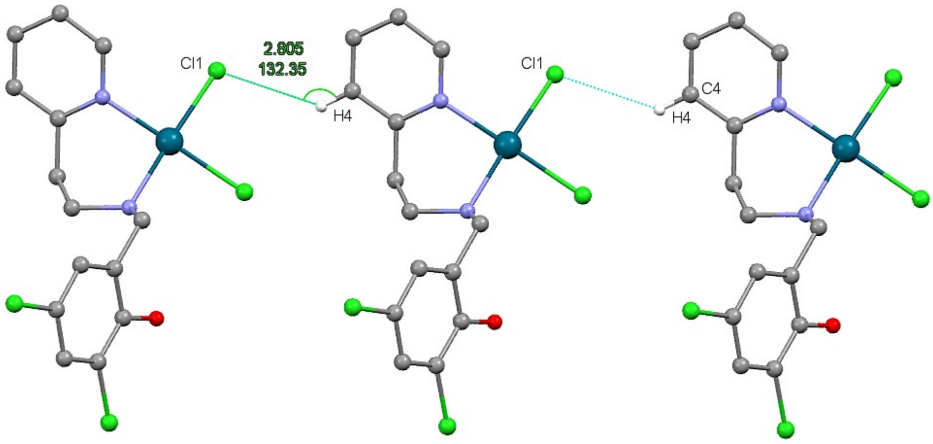

</td></tr>
<tr><td>

f

H-bonding
(C6-H6A…Cl4)

</td><td>

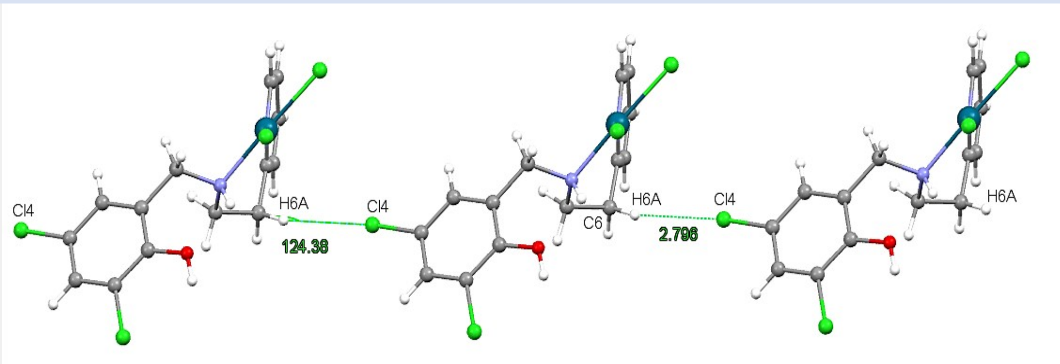

</td></tr>
</table>

g

H-bonding

(N2-H2A…O1-H1A…Cl1)
(H6A…Cl2…H2A)

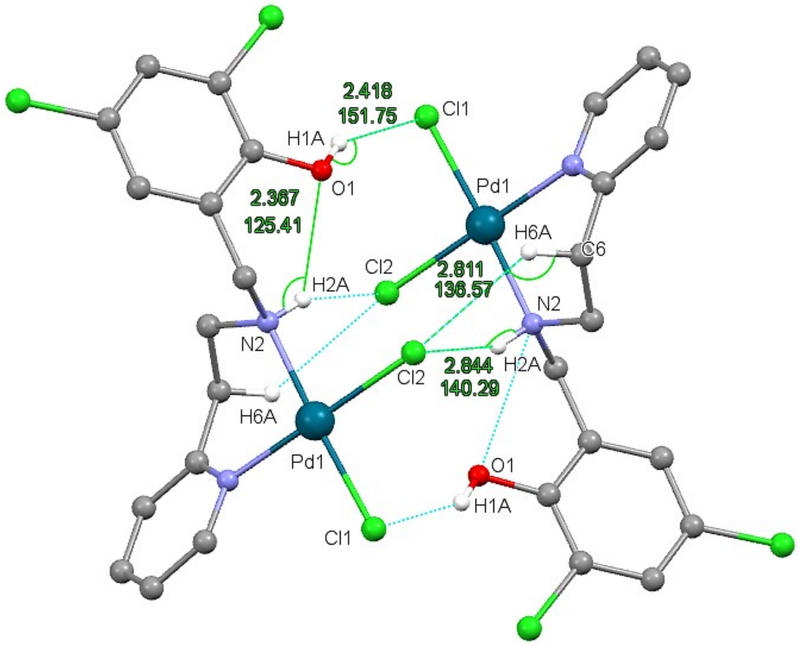

Fig. S4 Parts of the crystal packing of **Cl$_2$Py(R)Pd**, showing different aggregation patterns made by various intra- and intermolecular interactions. Intermolecular CH…π interactions (a), and various Intra- (b) and intermolecular hydrogen bonds (c-g), are represented.

Intra- and Intermolecular Interactions in crystal structure of ClBrPy(R)Pd

ClBrPy(R)Pd	
Intramolecular Interactions	
a **CH…π** ($_{aliphatic}$C7-H7A…C9$_{aromatic}$) ($_{aliphatic}$C7-H7B…C9$_{aromatic}$)	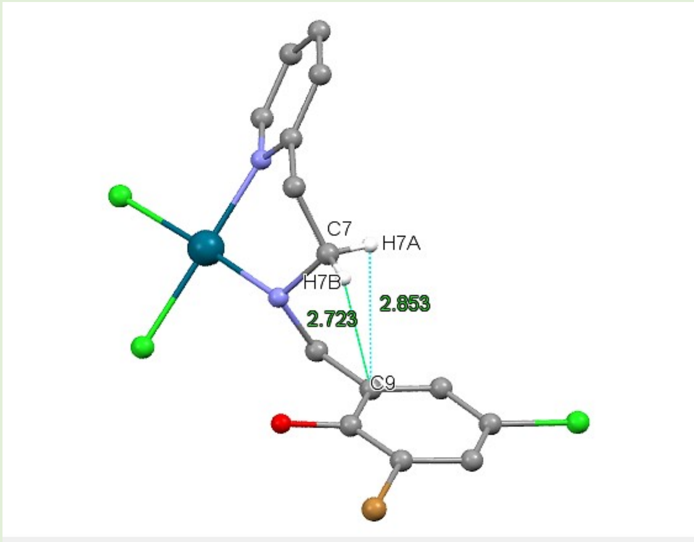
b **H-bonding** (C1-H1…Cl1) (C8-H8B…Cl2) (O1-H1A…Br1) (N2-H2A…O1)	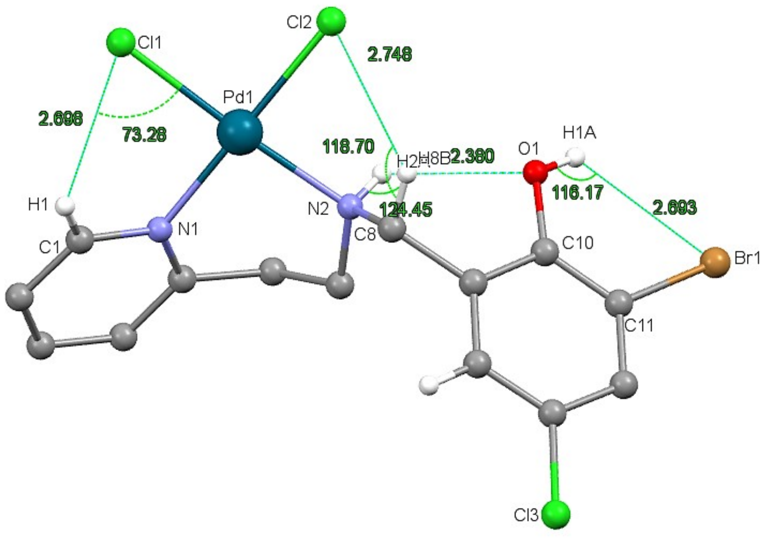
Intermolecular Interactions	

c **H-bonding** (C4-H4…Cl1)	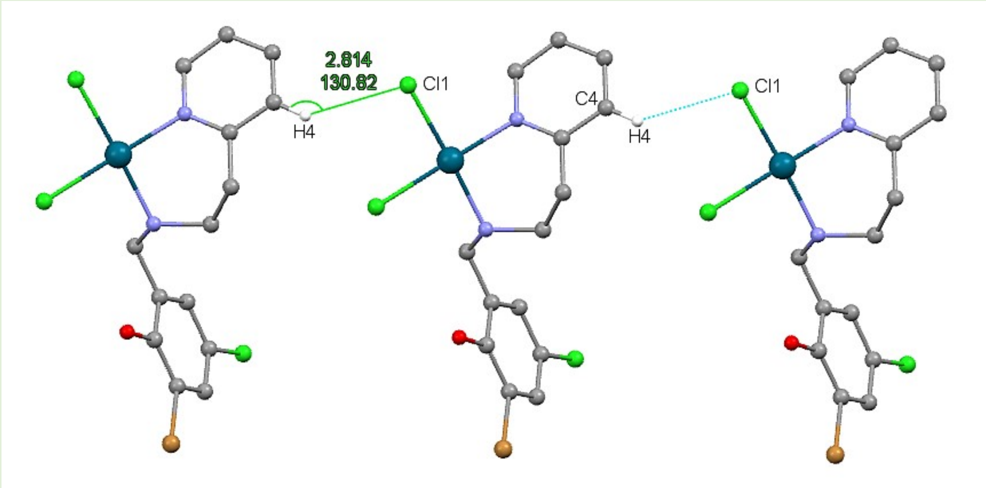
d **H-bonding** (C6-H6A…Cl3)	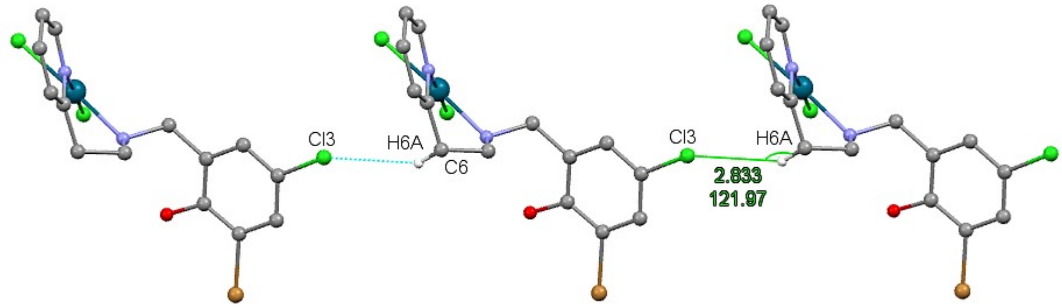
e **H-bonding** (C1-H1…Br1) **Halogen bond** (Cl1…Br1)	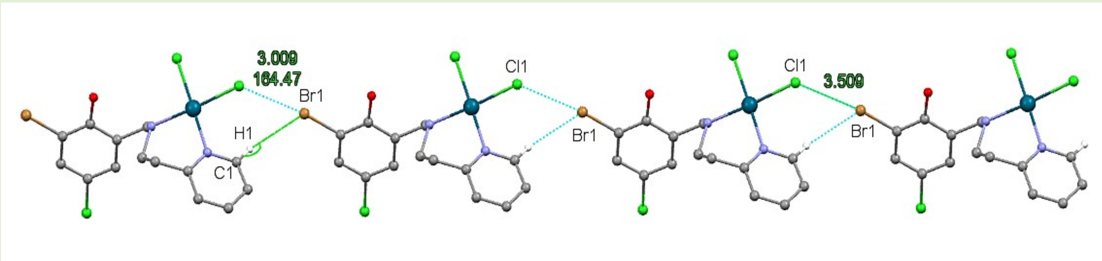

f

H-bonding

(O1-H1A…Cl1)

(H2A…Cl2…H6A)

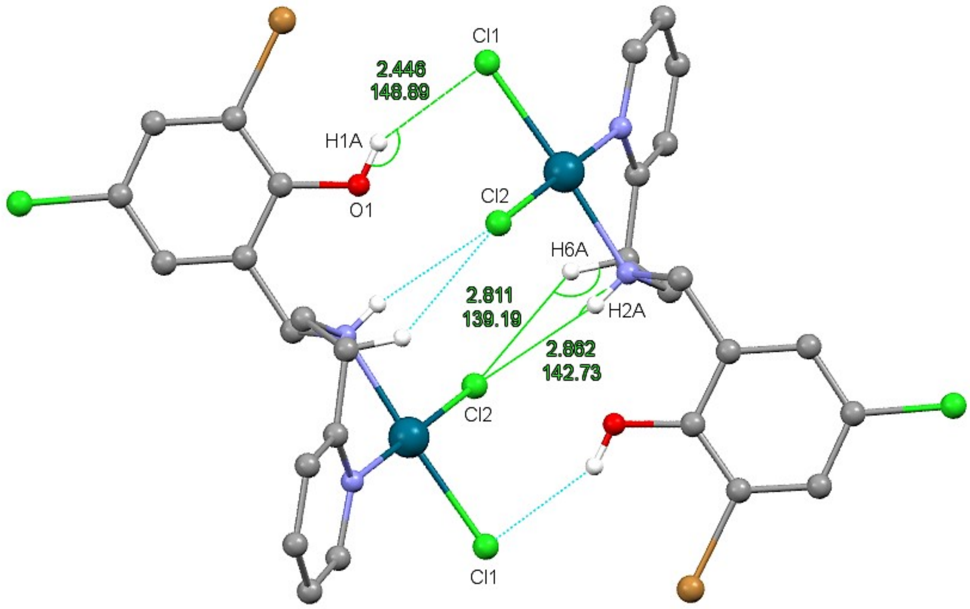

g

CH…π

($_{iminic}$C8H8B…C12$_{aromatic}$)

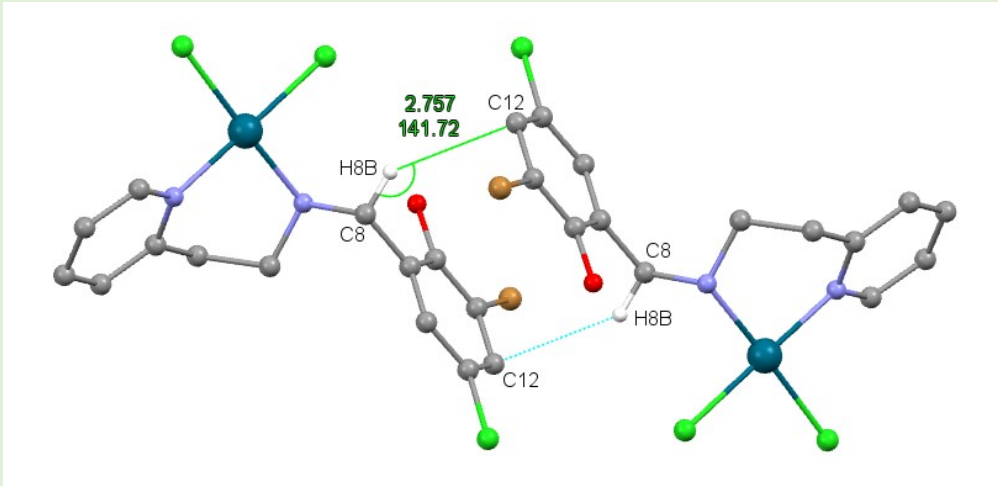

h

H-bonding

(C3-H3…Cl1)

π…π stacking

(C2…C2)

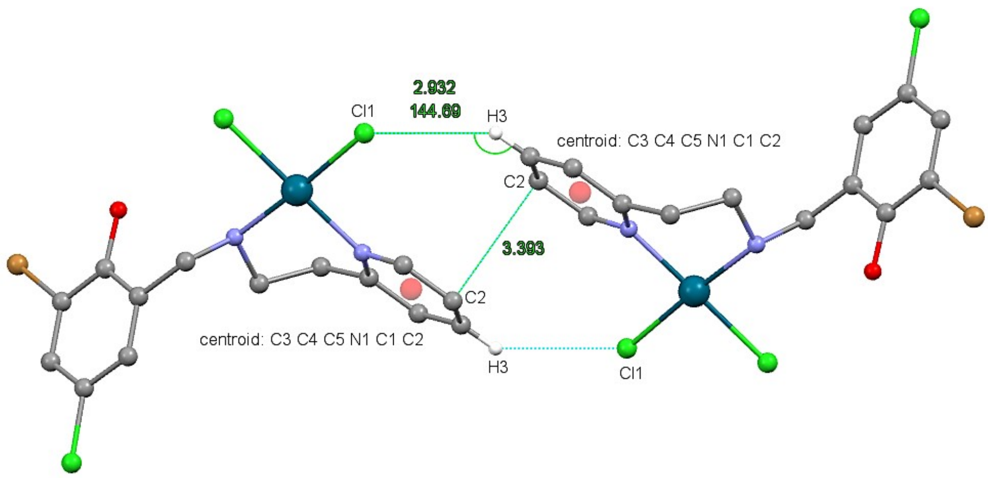

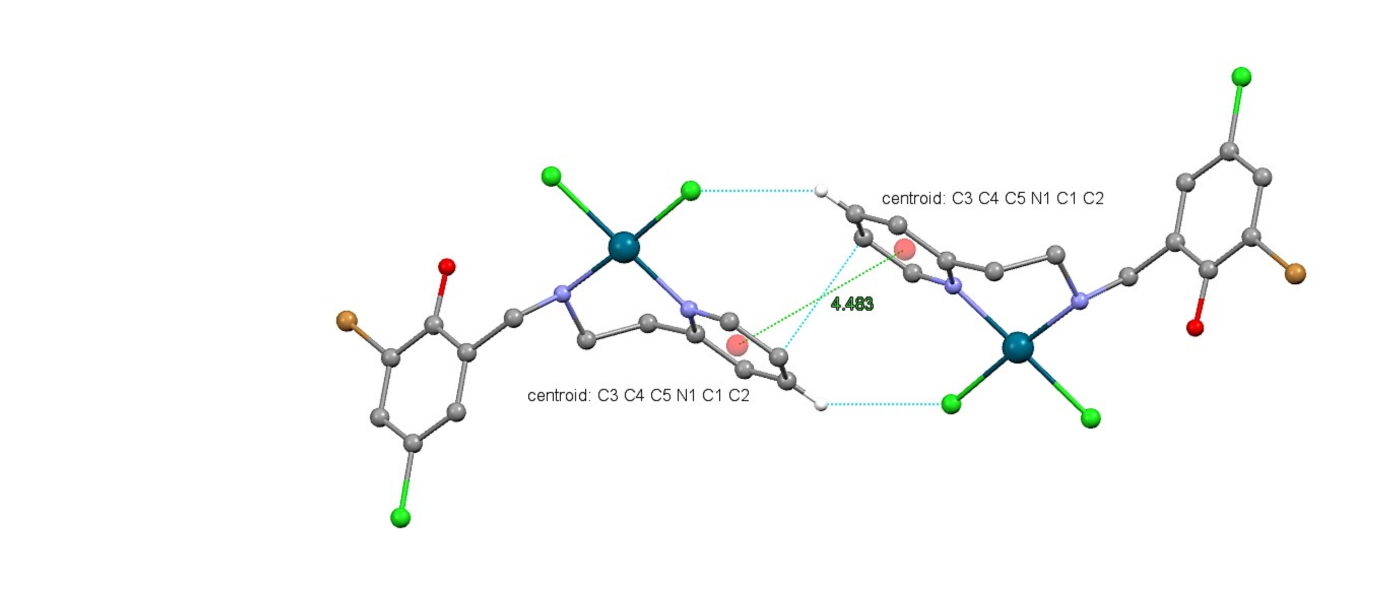

Fig. S5 Parts of the crystal packing of **ClBrPy(R)Pd**, showing different aggregation patterns made by various intra- and intermolecular interactions. Intra- (a) and intermolecular CH…π interactions (g), various intra- (b) and intermolecular hydrogen bonds (c-f, h), halogen bonds (e), and also π…π stacking interactions (h) are exhibited.

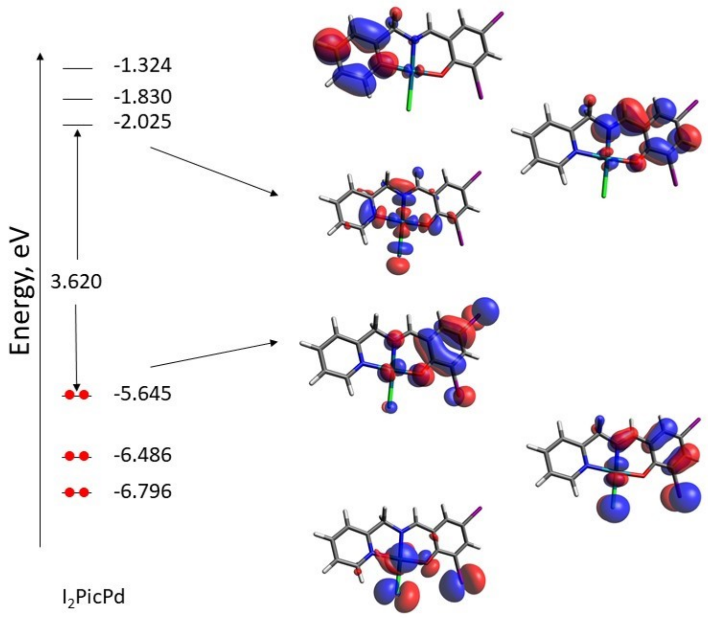

Fig. S6 Energy levels and isosurface contour plots for complex **I_2PicPd**.

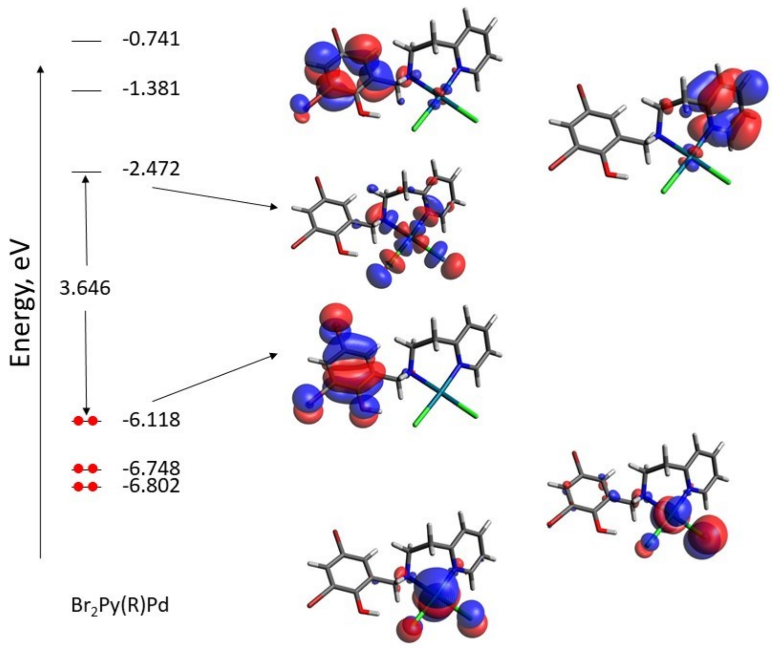

Fig. S7 Energy levels and isosurface contour plots for complex **Br_2Py(R)Pd**.

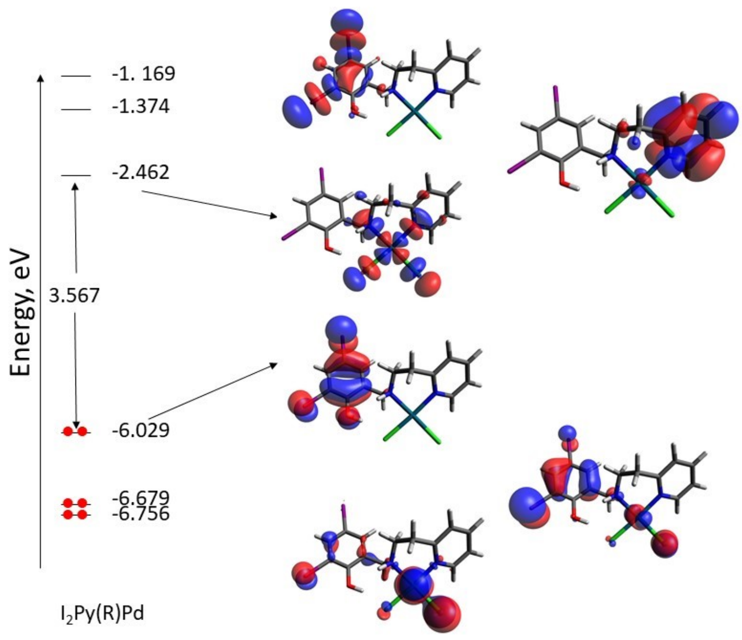

Fig. S8 Energy levels and isosurface contour plots for complex **I_2Py(R)Pd**.

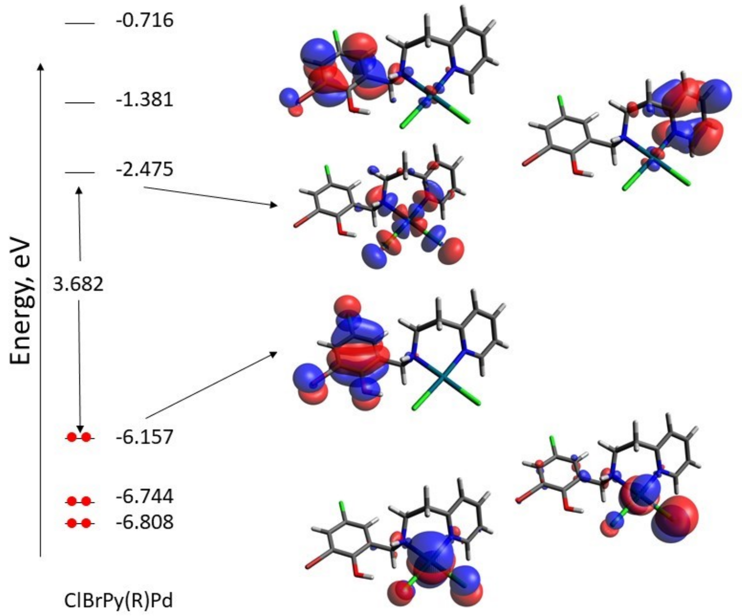

Fig. S9 Energy levels and isosurface contour plots for complex **ClBrPy(R)Pd**.

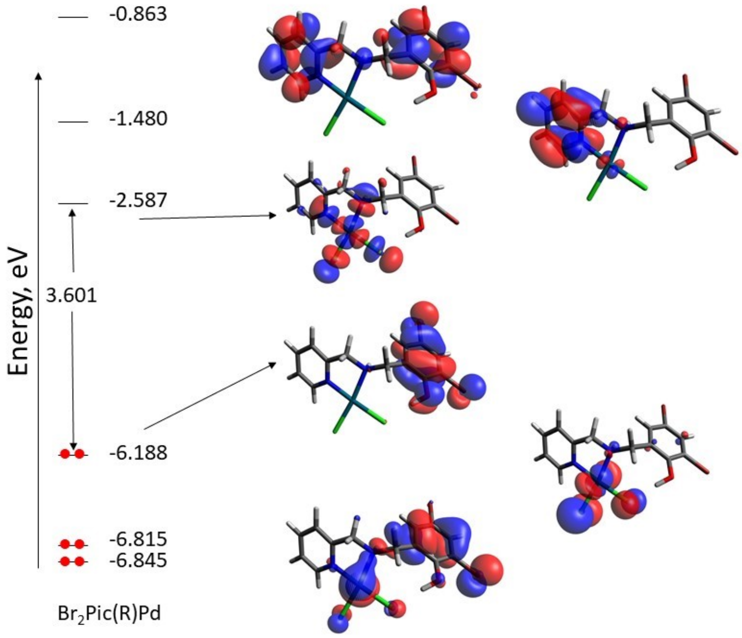

Fig. S10 Energy levels and isosurface contour plots for complex **Br$_2$Pic(R)Pd**.

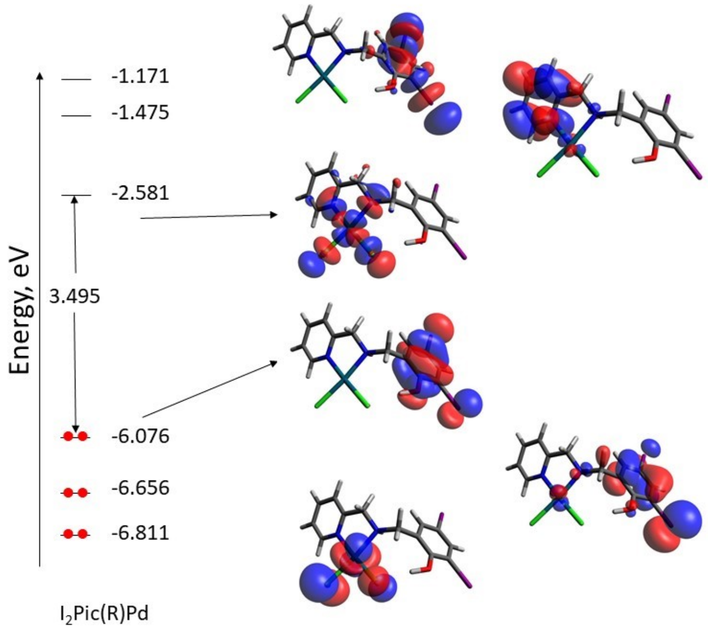

Fig. S11 Energy levels and isosurface contour plots for complex **I$_2$Pic(R)Pd**.

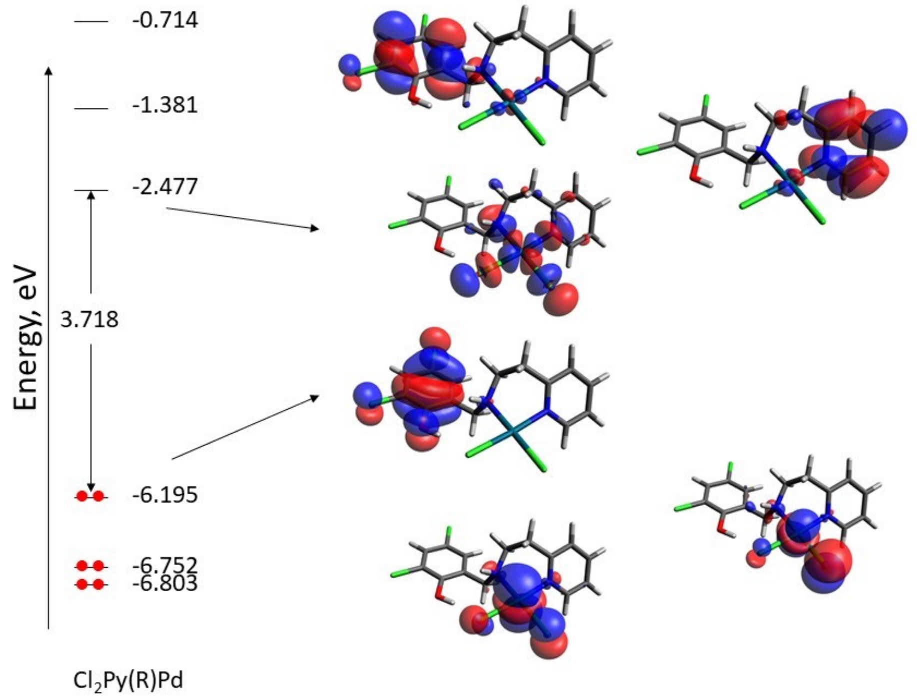

Fig. S12 Energy levels and isosurface contour plots for complex **Cl_2Py(R)Pd**.

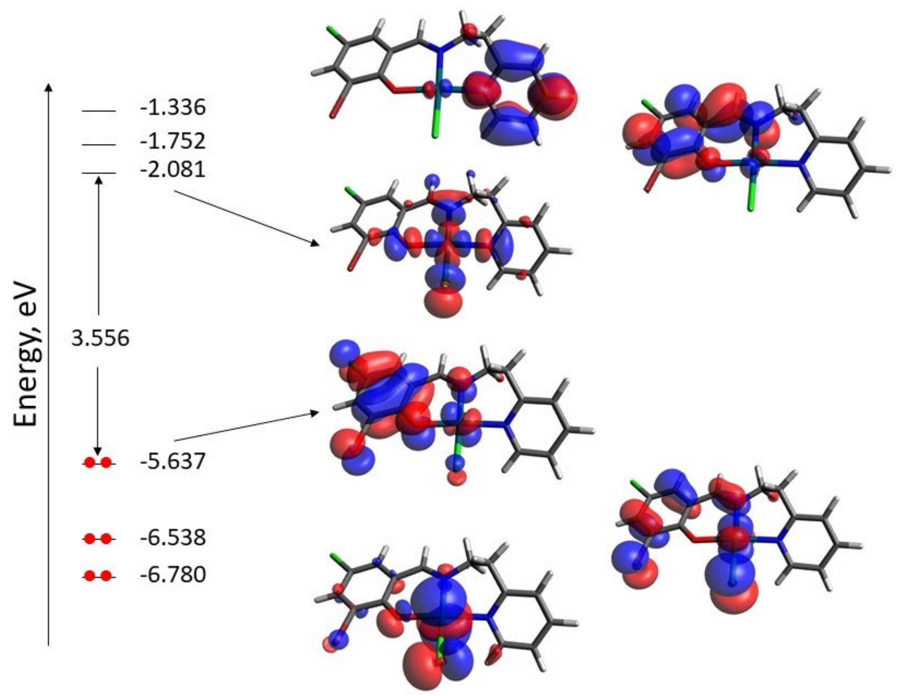

Fig. S13 Energy levels and isosurface contour plots for complex **ClBrPyPd**.

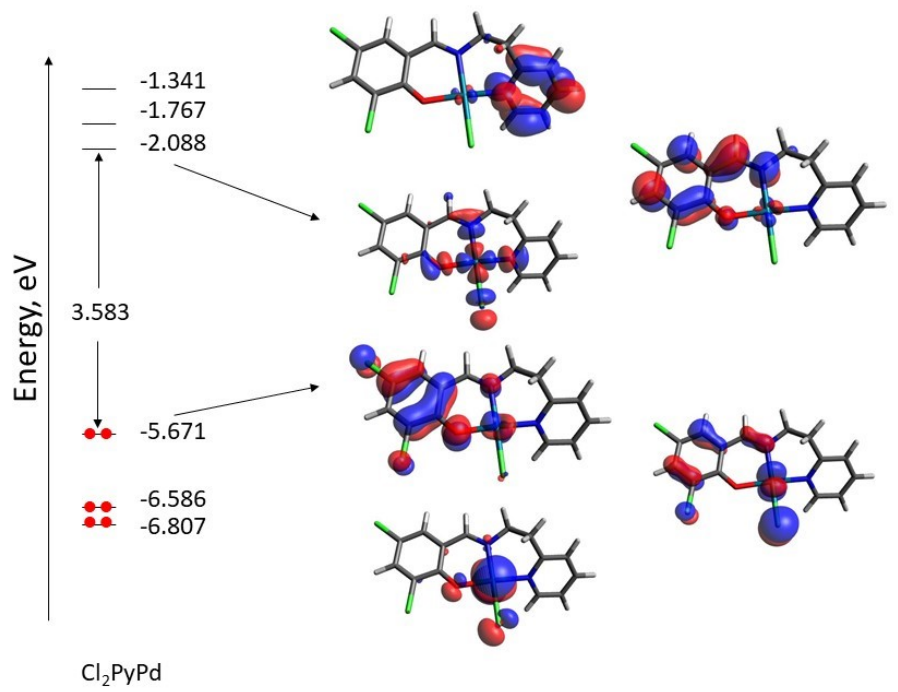

Fig. S14 Energy levels and isosurface contour plots for complex **Cl_2PyPd**.

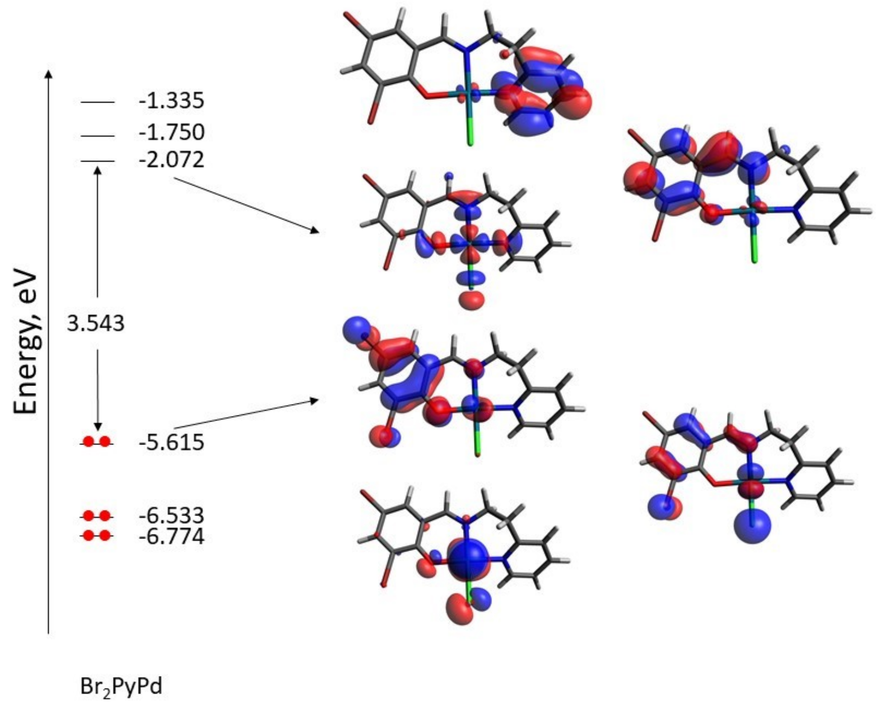

Fig. S15 Energy levels and isosurface contour plots for complex **Br_2PyPd**.

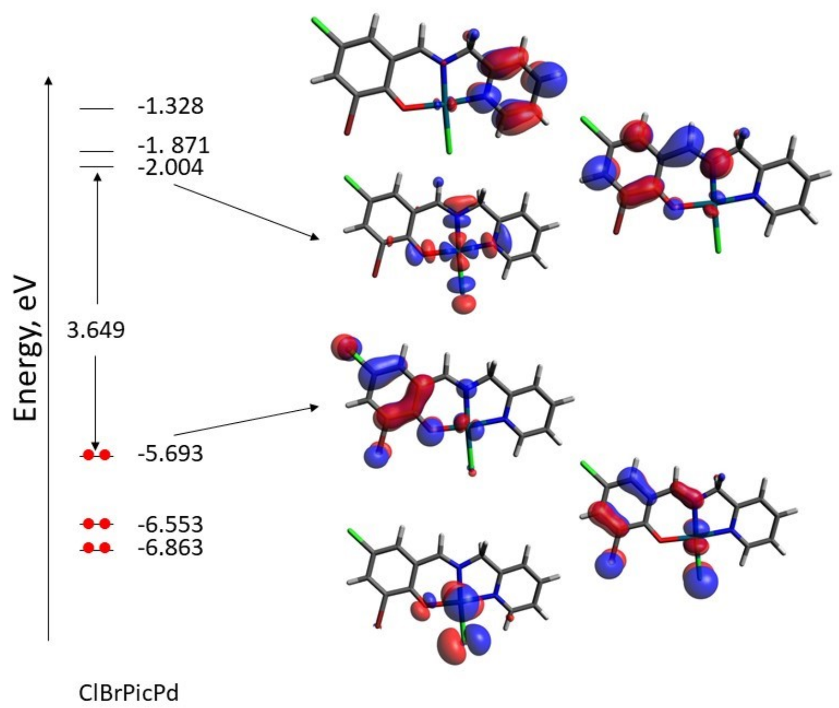

Fig. S16 Energy levels and isosurface contour plots for complex Cl**BrPicPd**.

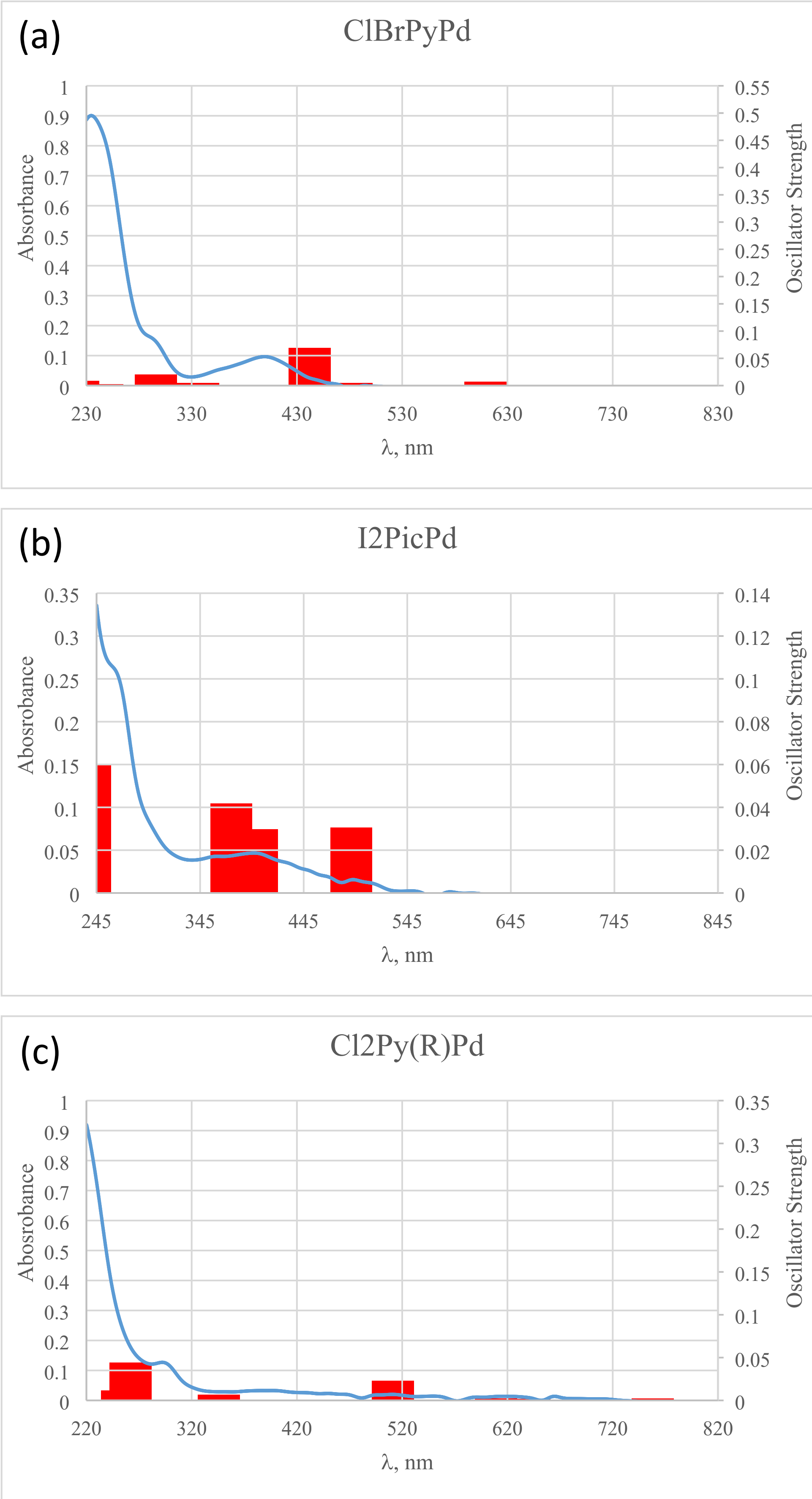
(a)
ClBrPyPd
Absorbance
Oscillator Strength
λ, nm
(b)
I2PicPd
Abosrobance
Oscillator Strength
λ, nm
(c)
Cl2Py(R)Pd
Abosrobance
Oscillator Strength
λ, nm

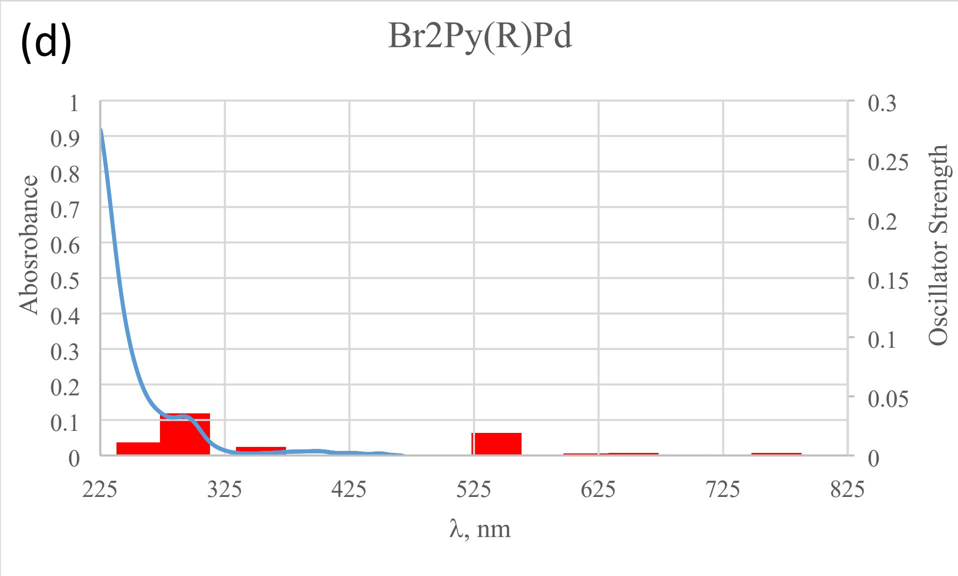
(d)
Br2Py(R)Pd
Abosrobance
Oscillator Strength
λ, nm
1
0.9
0.8
0.7
0.6
0.5
0.4
0.3
0.2
0.1
0
0.3
0.25
0.2
0.15
0.1
0.05
0
225
325
425
525
625
725
825

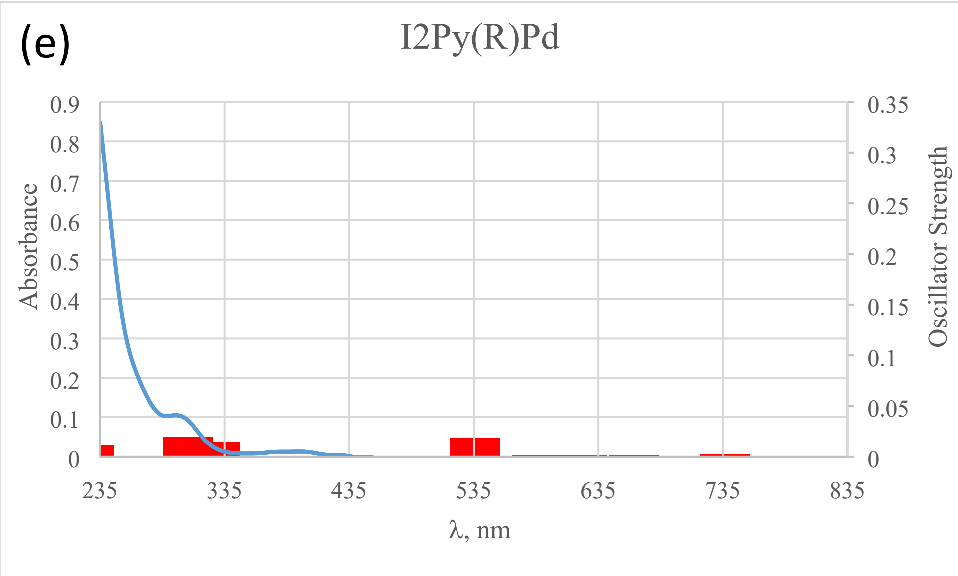
(e)
I2Py(R)Pd
Absorbance
Oscillator Strength
λ, nm
0.9
0.8
0.7
0.6
0.5
0.4
0.3
0.2
0.1
0
0.35
0.3
0.25
0.2
0.15
0.1
0.05
0
235
335
435
535
635
735
835

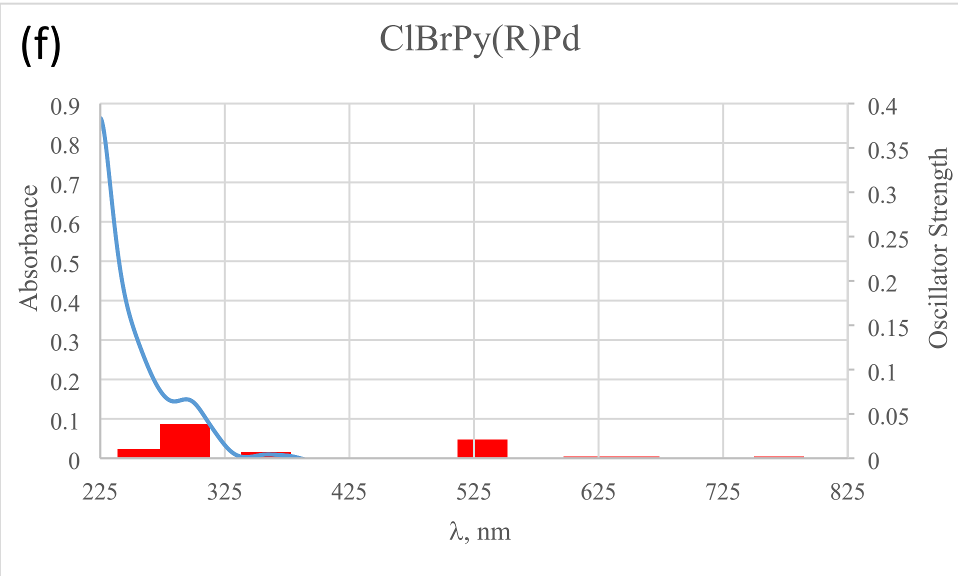
(f)
ClBrPy(R)Pd
Absorbance
Oscillator Strength
λ, nm
0.9
0.8
0.7
0.6
0.5
0.4
0.3
0.2
0.1
0
0.4
0.35
0.3
0.25
0.2
0.15
0.1
0.05
0
225
325
425
525
625
725
825

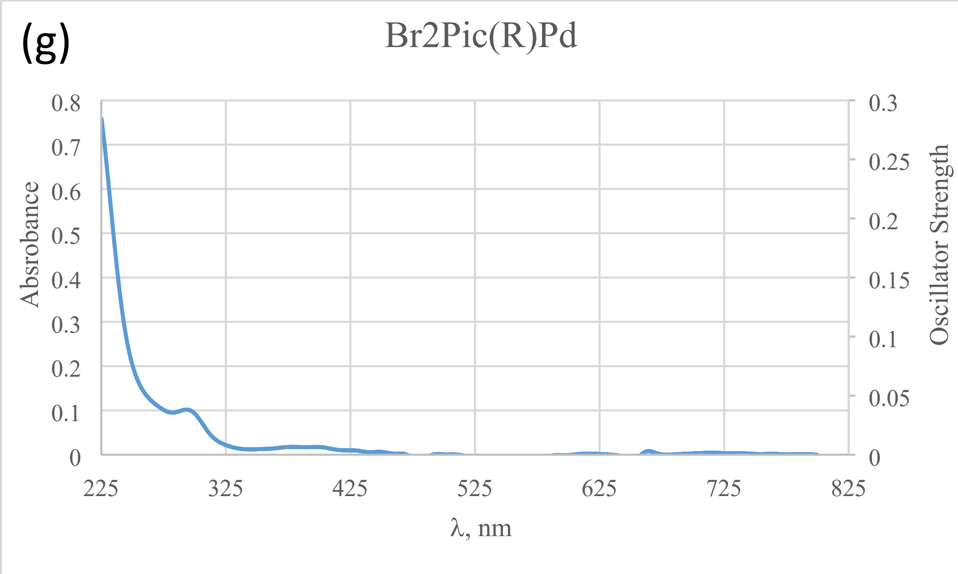

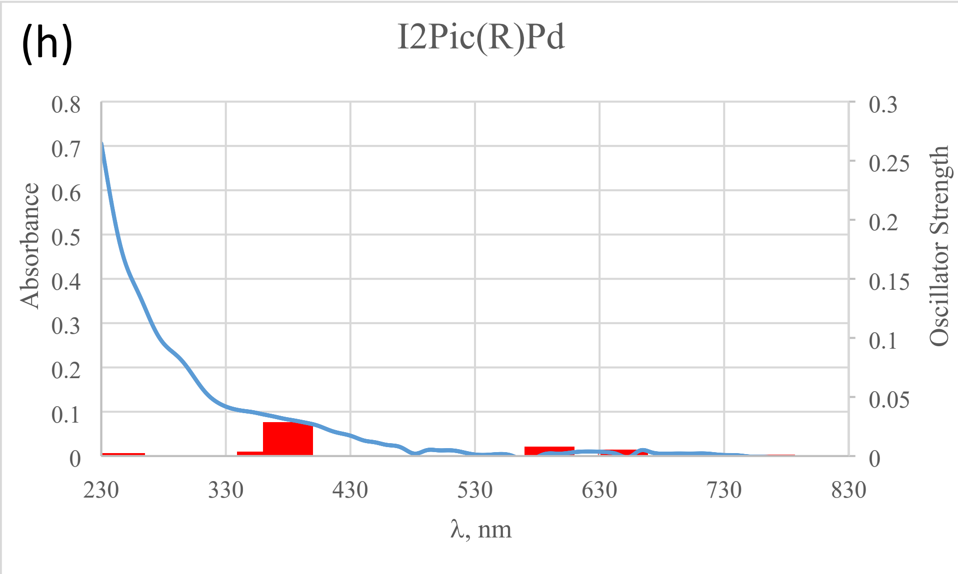

Fig. S17 Experimental absorption spectrum of complexes **ClBrPyPd** (a), **I_2PicPd** (b), **Cl_2Py(R)Pd** (c), **Br_2Py(R)Pd** (d), **I_2Py(R)Pd** (e), **ClBrPy(R)Pd** (f), **Br_2Pic(R)Pd** (g) and **I_2Pic(R)Pd** (h) in acetonitrile at 10 µM (blue line) and TD-DFT calculated singlet states (red lines).

Table S1 Lowest Singlet Excited States Calculated at the TDDFT B3LYP/(6-31G(d,p)+LANL2DZ) Level for Complex **I_2PicPd** in acetonitrile Solution[a]

Complex	Estate	Energy (eV)	λ (nm)	f.osc.	Monoexcitacions	Nature	Description
I_2PicPd	S_1	2.5863	479.39	0.0000	HOMO → LUMO (90)	$\pi_{sal} \rightarrow \sigma^*_{Pd-Cl} + \sigma^*_{Pd-N} + \sigma^*_{Pd-O}$	^{1}LMCT/^{1}LLCT/^{1}LC
	S_2	3.0492	406.62	0.0306	HOMO-4 → LUMO (27) HOMO-2 → LUMO (31) HOMO → LUMO+1 (35)	$d_\pi(Pd) + \pi_{Cl} \rightarrow \sigma^*_{Pd-Cl} + \sigma^*_{Pd-N} + \sigma^*_{Pd-O}$ $d_\pi(Pd) + \pi_{Cl} + \pi_I \rightarrow \sigma^*_{Pd-Cl} + \sigma^*_{Pd-N} + \sigma^*_{Pd-O}$ $\pi_{sal} \rightarrow \pi^*_{sal}$	^{1}MLCT/^{1}MC/^{1}LLCT/^{1}LC ^{1}MLCT/^{1}MC/^{1}LLCT/^{1}LC ^{1}LC
	S_3	3.1881	388.90	0.0001	HOMO-3 → LUMO (17) HOMO-1 → LUMO (67)	$d_\pi(Pd) + \pi_{Cl} \rightarrow \sigma^*_{Pd-Cl} + \sigma^*_{Pd-N} + \sigma^*_{Pd-O}$ $d_\pi(Pd) + \pi_{Cl} + \pi_I \rightarrow \sigma^*_{Pd-Cl} + \sigma^*_{Pd-N} + \sigma^*_{Pd-O}$	^{1}MLCT/^{1}MC/^{1}LLCT/^{1}LC ^{1}MLCT/^{1}MC/^{1}LLCT/^{1}LC
	S_4	3.2979	375.95	0.0298	HOMO-4 → LUMO (39) HOMO → LUMO+1 (55)	$d_\pi(Pd) + \pi_{Cl} \rightarrow \sigma^*_{Pd-Cl} + \sigma^*_{Pd-N} + \sigma^*_{Pd-O}$ $\pi_{sal} \rightarrow \pi^*_{sal}$	^{1}MLCT/^{1}MC/^{1}LLCT/^{1}LC ^{1}LC
	S_5	3.3718	367.70	0.0418	HOMO-4 → LUMO (27) HOMO-2 → LUMO (44)	$d_\pi(Pd) + \pi_{Cl} \rightarrow \sigma^*_{Pd-Cl} + \sigma^*_{Pd-N} + \sigma^*_{Pd-O}$ $d_\pi(Pd) + \pi_{Cl} + \pi_I \rightarrow \sigma^*_{Pd-Cl} + \sigma^*_{Pd-N} + \sigma^*_{Pd-O}$	^{1}MLCT/^{1}MC/^{1}LLCT/^{1}LC ^{1}MLCT/^{1}MC/^{1}LLCT/^{1}LC
	S_{13}	4.3328	286.15	0.1325	HOMO-5 → LUMO (76)	$d_\pi(Pd) + \pi_{Cl} + \pi_I \rightarrow \sigma^*_{Pd-Cl} + \sigma^*_{Pd-N} + \sigma^*_{Pd-O}$	^{1}MLCT/^{1}MC/^{1}LLCT/^{1}LC

[a] Vertical excitation energies (E), dominant monoexcitations with contributions (within parentheses) of >15%, the nature of the electronic transition, and the description of the excited state are summarized.

Table S2 Lowest Singlet Excited States Calculated at the TDDFT B3LYP/(6-31G(d,p)+LANL2DZ) Level for Complex **$Cl_2Py(R)Pd$** in acetonitrile Solution[a]

Complex	Estate	Energy (eV)	λ (nm)	f.osc.	Monoexcitacions	Nature	Description
$Cl_2Py(R)Pd$	S_1	2.6364	470.27	0.0020	HOMO-2 → LUMO (62)	$d_\pi(Pd) + \pi_{Cl} \rightarrow \sigma^*_{Pd-Cl} + \sigma^*_{Pd-N} + \sigma^*_{Pd-O}$	$^1MLCT/^1LLCT/^1LC$
					HOMO-1 → LUMO (38)	$d_\pi(Pd) + \pi_{Cl} \rightarrow \sigma^*_{Pd-Cl} + \sigma^*_{Pd-N} + \sigma^*_{Pd-O}$	$^1MLCT/^1LLCT/^1LC$
	S_2	2.7838	445.37	0.0009	HOMO-2 → LUMO (36)	$d_\pi(Pd) + \pi_{Cl} \rightarrow \sigma^*_{Pd-Cl} + \sigma^*_{Pd-N} + \sigma^*_{Pd-O}$	$^1MLCT/^1LLCT/^1LC$
					HOMO-1 → LUMO (56)	$d_\pi(Pd) + \pi_{Cl} \rightarrow \sigma^*_{Pd-Cl} + \sigma^*_{Pd-N} + \sigma^*_{Pd-O}$	$^1MLCT/^1LLCT/^1LC$
	S_3	2.8780	430.80	0.0018	HOMO-4 → LUMO (32)	$d_\pi(Pd) + \pi_{Cl} \rightarrow \sigma^*_{Pd-Cl} + \sigma^*_{Pd-N} + \sigma^*_{Pd-O}$	$^1MLCT/^1LLCT/^1LC$
					HOMO-3 → LUMO (52)	$d_\pi(Pd) + \pi_{Cl} \rightarrow \sigma^*_{Pd-Cl} + \sigma^*_{Pd-N} + \sigma^*_{Pd-O}$	$^1MLCT/^1LLCT/^1LC$
	S_4	2.9533	419.81	0.0021	HOMO-4 → LUMO (65)	$d_\pi(Pd) + \pi_{Cl} \rightarrow \sigma^*_{Pd-Cl} + \sigma^*_{Pd-N} + \sigma^*_{Pd-O}$	$^1MLCT/^1LLCT/^1LC$
					HOMO-3 → LUMO (23)	$d_\pi(Pd) + \pi_{Cl} \rightarrow \sigma^*_{Pd-Cl} + \sigma^*_{Pd-N} + \sigma^*_{Pd-O}$	$^1MLCT/^1LLCT/^1LC$
	S_5	3.2027	387.13	0.0227	HOMO → LUMO (100)	$\pi_{Cl2PhOH} \rightarrow \sigma^*_{Pd-Cl} + \sigma^*_{Pd-N} + \sigma^*_{Pd-O}$	$^1LMCT/^1LLCT/^1LC$
	S_{18}	5.1216	242.08	0.3243	HOMO-9 → LUMO (15)	$\pi_{Cl} + \pi_{py} \rightarrow \sigma^*_{Pd-Cl} + \sigma^*_{Pd-N} + \sigma^*_{Pd-O}$	$^1LMCT/^1LLCT/^1LC$
					HOMO-8 → LUMO (47)	$d_\pi(Pd) + \pi_{Cl} + \pi_{py} \rightarrow \sigma^*_{Pd-Cl} + \sigma^*_{Pd-N} + \sigma^*_{Pd-O}$	$^1MLCT/^1LLCT/^1LC$

[a] Vertical excitation energies (E), dominant monoexcitations with contributions (within parentheses) of >15%, the nature of the electronic transition, and the description of the excited state are summarized.

Table S3 Lowest Singlet Excited States Calculated at the TDDFT B3LYP/(6-31G(d,p)+LANL2DZ) Level for Complex **Br_2Py(R)Pd** in acetonitrile Solution[a]

Complex	Estate	Energy (eV)	λ (nm)	f.osc.	Monoexcitacions	Nature	Description
Br_2Py(R)Pd	S_1	2.6424	469.20	0.0020	HOMO-2 → LUMO (66) HOMO-1 → LUMO (34)	d_π(Pd) + π_{Cl} → $\sigma^*_{Pd\text{-}Cl}$ + $\sigma^*_{Pd\text{-}N}$+ $\sigma^*_{Pd\text{-}O}$ d_π(Pd) + π_{Cl} → $\sigma^*_{Pd\text{-}Cl}$ + $\sigma^*_{Pd\text{-}N}$+ $\sigma^*_{Pd\text{-}O}$	^{1}MLCT/^{1}LLCT/^{1}LC ^{1}MLCT/^{1}LLCT/^{1}LC
	S_2	2.7886	444.62	0.0010	HOMO-2 → LUMO (32) HOMO-1 → LUMO (58)	d_π(Pd) + π_{Cl} → $\sigma^*_{Pd\text{-}Cl}$ + $\sigma^*_{Pd\text{-}N}$+ $\sigma^*_{Pd\text{-}O}$ d_π(Pd) + π_{Cl} → $\sigma^*_{Pd\text{-}Cl}$ + $\sigma^*_{Pd\text{-}N}$+ $\sigma^*_{Pd\text{-}O}$	^{1}MLCT/^{1}LLCT/^{1}LC ^{1}MLCT/^{1}LLCT/^{1}LC
	S_3	2.8785	430.73	0.0019	HOMO-5 → LUMO (31) HOMO-3 → LUMO (51)	d_π(Pd) + π_{Cl} → $\sigma^*_{Pd\text{-}Cl}$ + $\sigma^*_{Pd\text{-}N}$+ $\sigma^*_{Pd\text{-}O}$ d_π(Pd) + π_{Cl} → $\sigma^*_{Pd\text{-}Cl}$ + $\sigma^*_{Pd\text{-}N}$+ $\sigma^*_{Pd\text{-}O}$	^{1}MLCT/^{1}LLCT/^{1}LC ^{1}MLCT/^{1}LLCT/^{1}LC
	S_4	2.9584	419.09	0.0018	HOMO-5 → LUMO (64) HOMO-3 → LUMO (21)	d_π(Pd) + π_{Cl} → $\sigma^*_{Pd\text{-}Cl}$ + $\sigma^*_{Pd\text{-}N}$+ $\sigma^*_{Pd\text{-}O}$ d_π(Pd) + π_{Cl} → $\sigma^*_{Pd\text{-}Cl}$ + $\sigma^*_{Pd\text{-}N}$+ $\sigma^*_{Pd\text{-}O}$	^{1}MLCT/^{1}LLCT/^{1}LC ^{1}MLCT/^{1}LLCT/^{1}LC
	S_5	3.1430	394.48	0.0191	HOMO → LUMO (100)	$\pi_{Br2PhOH}$ → $\sigma^*_{Pd\text{-}Cl}$ + $\sigma^*_{Pd\text{-}N}$+ $\sigma^*_{Pd\text{-}O}$	^{1}LMCT/^{1}LLCT/^{1}LC
	S_{30}	5.4606	227.05	0.2835	HOMO-17 → LUMO (21) HOMO-14 → LUMO (23) HOMO → LUMO+5 (38)	d_π(Pd) + π_{Cl} + π_{py} → $\sigma^*_{Pd\text{-}Cl}$ + $\sigma^*_{Pd\text{-}N}$+ $\sigma^*_{Pd\text{-}O}$ d_π(Pd) + π_{Cl} + π_{py} → $\sigma^*_{Pd\text{-}Cl}$ + $\sigma^*_{Pd\text{-}N}$+ $\sigma^*_{Pd\text{-}O}$ $\pi_{Br2PhOH}$ → $\pi^*_{Br2PhOH)}$	^{1}MLCT/^{1}LLCT/^{1}LC ^{1}MLCT/^{1}LLCT/^{1}LC ^{1}LC

[a] Vertical excitation energies (E), dominant monoexcitations with contributions (within parentheses) of >15%, the nature of the electronic transition, and the description of the excited state are summarized.

Table S4 Lowest Singlet Excited States Calculated at the TDDFT B3LYP/(6-31G(d,p)+LANL2DZ) Level for Complex **I_2Py(R)Pd** in acetonitrile Solution[a]

Complex	Estate	Energy (eV)	λ (nm)	f.osc.	Monoexcitacions	Nature	Description
I_2Py(R)Pd	S_1	2.6426	469.18	0.0023	HOMO-3 → LUMO (46)	$d_\pi(Pd) + \pi_{Cl} \rightarrow \sigma^*_{Pd\text{-}Cl} + \sigma^*_{Pd\text{-}N} + \sigma^*_{Pd\text{-}O}$	^{1}MLCT/^{1}LLCT/^{1}LC
					HOMO-2 → LUMO (51)	$d_\pi(Pd) + \pi_{Cl} \rightarrow \sigma^*_{Pd\text{-}Cl} + \sigma^*_{Pd\text{-}N} + \sigma^*_{Pd\text{-}O}$	^{1}MLCT/^{1}LLCT/^{1}LC
	S_2	2.7887	444.59	0.0013	HOMO-3 → LUMO (48)	$d_\pi(Pd) + \pi_{Cl} \rightarrow \sigma^*_{Pd\text{-}Cl} + \sigma^*_{Pd\text{-}N} + \sigma^*_{Pd\text{-}O}$	^{1}MLCT/^{1}LLCT/^{1}LC
					HOMO-2 → LUMO (28)	$d_\pi(Pd) + \pi_{Cl} \rightarrow \sigma^*_{Pd\text{-}Cl} + \sigma^*_{Pd\text{-}N} + \sigma^*_{Pd\text{-}O}$	^{1}MLCT/^{1}LLCT/^{1}LC
					HOMO-1 → LUMO (18)	$\pi_{Br2PhOH} \rightarrow \sigma^*_{Pd\text{-}Cl} + \sigma^*_{Pd\text{-}N} + \sigma^*_{Pd\text{-}O}$	^{1}LMCT/^{1}LLCT/^{1}LC
	S_3	2.8783	430.76	0.0018	HOMO-5 → LUMO (34)	$d_\pi(Pd) + \pi_{Cl} \rightarrow \sigma^*_{Pd\text{-}Cl} + \sigma^*_{Pd\text{-}N} + \sigma^*_{Pd\text{-}O}$	^{1}MLCT/^{1}LLCT/^{1}LC
					HOMO-4 → LUMO (53)	$d_\pi(Pd) + \pi_{Cl} \rightarrow \sigma^*_{Pd\text{-}Cl} + \sigma^*_{Pd\text{-}N} + \sigma^*_{Pd\text{-}O}$	^{1}MLCT/^{1}LLCT/^{1}LC
	S_4	2.9572	419.26	0.0018	HOMO-5 → LUMO (65)	$d_\pi(Pd) + \pi_{Cl} \rightarrow \sigma^*_{Pd\text{-}Cl} + \sigma^*_{Pd\text{-}N} + \sigma^*_{Pd\text{-}O}$	^{1}MLCT/^{1}LLCT/^{1}LC
					HOMO-4 → LUMO (22)	$d_\pi(Pd) + \pi_{Cl} \rightarrow \sigma^*_{Pd\text{-}Cl} + \sigma^*_{Pd\text{-}N} + \sigma^*_{Pd\text{-}O}$	^{1}MLCT/^{1}LLCT/^{1}LC
	S_5	3.0782	402.79	0.0184	HOMO → LUMO (100)	$\pi_{I2PhOH} \rightarrow \sigma^*_{Pd\text{-}Cl} + \sigma^*_{Pd\text{-}N} + \sigma^*_{Pd\text{-}O}$	^{1}LMCT/^{1}LLCT/^{1}LC
	S_{27}	5.1347	241.46	0.3220	HOMO-13 → LUMO (17)	$d_\pi(Pd) + \pi_{Cl} + \pi_{py} \rightarrow \sigma^*_{Pd\text{-}Cl} + \sigma^*_{Pd\text{-}N} + \sigma^*_{Pd\text{-}O}$	^{1}MLCT/^{1}LLCT/^{1}LC
					HOMO-11 → LUMO (44)	$d_\pi(Pd) + \pi_{Cl} + \pi_{py} \rightarrow \sigma^*_{Pd\text{-}Cl} + \sigma^*_{Pd\text{-}N} + \sigma^*_{Pd\text{-}O}$	^{1}MLCT/^{1}LLCT/^{1}LC

[a] Vertical excitation energies (E), dominant monoexcitations with contributions (within parentheses) of >15%, the nature of the electronic transition, and the description of the excited state are summarized.

Table S5 Lowest Singlet Excited States Calculated at the TDDFT B3LYP/(6-31G(d,p)+LANL2DZ) Level for Complex **ClBrPy(R)Pd** in acetonitrile Solution[a]

Complex	Estate	Energy (eV)	λ (nm)	f.osc.	Monoexcitacions	Nature	Description
ClBrPy(R)Pd	S_1	2.6400	469.64	0.0021	HOMO-2 → LUMO (61)	$d_\pi(Pd) + \pi_{Cl} \rightarrow \sigma^*_{Pd-Cl} + \sigma^*_{Pd-N} + \sigma^*_{Pd-O}$	^{1}MLCT/^{1}LLCT/^{1}LC
					HOMO-1 → LUMO (39)	$d_\pi(Pd) + \pi_{Cl} \rightarrow \sigma^*_{Pd-Cl} + \sigma^*_{Pd-N} + \sigma^*_{Pd-O}$	^{1}MLCT/^{1}LLCT/^{1}LC
	S_2	2.7870	444.87	0.0011	HOMO-2 → LUMO (37)	$d_\pi(Pd) + \pi_{Cl} \rightarrow \sigma^*_{Pd-Cl} + \sigma^*_{Pd-N} + \sigma^*_{Pd-O}$	^{1}MLCT/^{1}LLCT/^{1}LC
					HOMO-1 → LUMO (54)	$d_\pi(Pd) + \pi_{Cl} \rightarrow \sigma^*_{Pd-Cl} + \sigma^*_{Pd-N} + \sigma^*_{Pd-O}$	^{1}MLCT/^{1}LLCT/^{1}LC
	S_3	2.8755	431.18	0.0019	HOMO-5 → LUMO (29)	$d_\pi(Pd) + \pi_{Cl} \rightarrow \sigma^*_{Pd-Cl} + \sigma^*_{Pd-N} + \sigma^*_{Pd-O}$	^{1}MLCT/^{1}LLCT/^{1}LC
					HOMO-3 → LUMO (53)	$d_\pi(Pd) + \pi_{Cl} \rightarrow \sigma^*_{Pd-Cl} + \sigma^*_{Pd-N} + \sigma^*_{Pd-O}$	^{1}MLCT/^{1}LLCT/^{1}LC
	S_4	2.9580	419.14	0.0019	HOMO-5 → LUMO (69)	$d_\pi(Pd) + \pi_{Cl} \rightarrow \sigma^*_{Pd-Cl} + \sigma^*_{Pd-N} + \sigma^*_{Pd-O}$	^{1}MLCT/^{1}LLCT/^{1}LC
					HOMO-3 → LUMO (21)	$d_\pi(Pd) + \pi_{Cl} \rightarrow \sigma^*_{Pd-Cl} + \sigma^*_{Pd-N} + \sigma^*_{Pd-O}$	^{1}MLCT/^{1}LLCT/^{1}LC
	S_5	3.1716	390.92	0.0209	HOMO → LUMO (100)	$\pi_{ClBrPhOH} \rightarrow \sigma^*_{Pd-Cl} + \sigma^*_{Pd-N} + \sigma^*_{Pd-O}$	^{1}LMCT/^{1}LLCT/^{1}LC
	S_{29}	5.4763	226.40	0.3392	HOMO-17 → LUMO (23)	$d_\pi(Pd) + \pi_{Cl} + \pi_{py} \rightarrow \sigma^*_{Pd-Cl} + \sigma^*_{Pd-N} + \sigma^*_{Pd-O}$	^{1}MLCT/^{1}LLCT/^{1}LC
					HOMO-13 → LUMO (51)	$d_\pi(Pd) + \pi_{Cl} + \pi_{py} \rightarrow \sigma^*_{Pd-Cl} + \sigma^*_{Pd-N} + \sigma^*_{Pd-O}$	^{1}MLCT/^{1}LLCT/^{1}LC

[a] Vertical excitation energies (E), dominant monoexcitations with contributions (within parentheses) of >15%, the nature of the electronic transition, and the description of the excited state are summarized.

Table S6 Lowest Singlet Excited States Calculated at the TDDFT B3LYP/(6-31G(d,p)+LANL2DZ) Level for Complex **Br_2Pic(R)Pd** in acetonitrile Solution[a]

Complex	Estate	Energy (eV)	λ (nm)	f.osc.	Monoexcitacions	Nature	Description
Br_2Pic(R)Pd	S_1	2.6199	473.24	0.0007	HOMO-3 → LUMO (61) HOMO-2 → LUMO (23)	$d_{\pi}(Pd) + \pi_{Cl} + \pi_{ar} \rightarrow \sigma^*_{Pd-Cl} + \sigma^*_{Pd-N} + \sigma^*_{Pd-O}$ $d_{\pi}(Pd) + \pi_{Cl} + \pi_{ar} \rightarrow \sigma^*_{Pd-Cl} + \sigma^*_{Pd-N} + \sigma^*_{Pd-O}$	^{1}MLCT/^{1}LC ^{1}MLCT/^{1}LC
	S_2	2.7151	456.64	0.0001	HOMO-1 → LUMO (81)	$d_{\pi}(Pd) + \pi_{Cl} \rightarrow \sigma^*_{Pd-Cl} + \sigma^*_{Pd-N} + \sigma^*_{Pd-O}$	^{1}MLCT/^{1}LLCT/^{1}LC
	S_3	2.8100	441.23	0.0001	HOMO-4 → LUMO (86)	$d_{\pi}(Pd) + \pi_{Cl} \rightarrow \sigma^*_{Pd-Cl} + \sigma^*_{Pd-N} + \sigma^*_{Pd-O}$	^{1}MLCT/^{1}LLCT/^{1}LC
	S_4	2.8567	434.01	0.0048	HOMO-6 → LUMO (19) HOMO-5 → LUMO (52)	$d_{\pi}(Pd) + \pi_{Cl} \rightarrow \sigma^*_{Pd-Cl} + \sigma^*_{Pd-N} + \sigma^*_{Pd-O}$ $d_{\pi}(Pd) + \pi_{Cl} \rightarrow \sigma^*_{Pd-Cl} + \sigma^*_{Pd-N} + \sigma^*_{Pd-O}$	^{1}MLCT/^{1}LLCT/^{1}LC ^{1}MLCT/^{1}LLCT/^{1}LC
	S_5	3.0699	403.87	0.0105	HOMO → LUMO (100)	$\pi_{Br2PhOH} \rightarrow \sigma^*_{Pd-Cl} + \sigma^*_{Pd-N} + \sigma^*_{Pd-O}$	^{1}LMCT/^{1}LLCT/^{1}LC
	S_{25}	5.2580	235.80	0.2661	HOMO-12 → LUMO (46)	$d_{\pi}(Pd) + \pi_{Cl} \rightarrow \sigma^*_{Pd-Cl} + \sigma^*_{Pd-N} + \sigma^*_{Pd-O}$	^{1}MLCT/^{1}LLCT/^{1}LC

[a] Vertical excitation energies (E), dominant monoexcitations with contributions (within parentheses) of >15%, the nature of the electronic transition, and the description of the excited state are summarized.

Table S7 Lowest Singlet Excited States Calculated at the TDDFT B3LYP/(6-31G(d,p)+LANL2DZ) Level for Complex **I_2Pic(R)Pd** in acetonitrile Solution[a]

Complex	Estate	Energy (eV)	λ (nm)	f.osc.	Monoexcitacions	Nature	Description
I_2Pic(R)Pd	S_1	2.6171	473.75	0.0009	HOMO-3 → LUMO (97)	$d_{\pi}(Pd)_r \rightarrow \sigma^*_{Pd-Cl} + \sigma^*_{Pd-N} + \sigma^*_{Pd-O}$	^{1}MLCT
	S_2	2.7089	457.69	0.0002	HOMO-2 → LUMO (94)	$d_{\pi}(Pd) + \pi_{Cl} \rightarrow \sigma^*_{Pd-Cl} + \sigma^*_{Pd-N} + \sigma^*_{Pd-O}$	^{1}MLCT/^{1}LLCT/^{1}LC
	S_3	2.8074	441.64	0.0002	HOMO-5 → LUMO (17) HOMO-4 → LUMO (76)	$d_{\pi}(Pd) + \pi_{Cl} \rightarrow \sigma^*_{Pd-Cl} + \sigma^*_{Pd-N} + \sigma^*_{Pd-O}$ $d_{\pi}(Pd) + \pi_{Cl} \rightarrow \sigma^*_{Pd-Cl} + \sigma^*_{Pd-N} + \sigma^*_{Pd-O}$	^{1}MLCT/^{1}LLCT/^{1}LC ^{1}MLCT/^{1}LLCT/^{1}LC
	S_4	2.8506	434.94	0.0051	HOMO-5 → LUMO (57) HOMO-4 → LUMO (15)	$d_{\pi}(Pd) + \pi_{Cl} \rightarrow \sigma^*_{Pd-Cl} + \sigma^*_{Pd-N} + \sigma^*_{Pd-O}$ $d_{\pi}(Pd) + \pi_{Cl} \rightarrow \sigma^*_{Pd-Cl} + \sigma^*_{Pd-N} + \sigma^*_{Pd-O}$	^{1}MLCT/^{1}LLCT/^{1}LC ^{1}MLCT/^{1}LLCT/^{1}LC
	S_5	2.9846	415.41	0.0078	HOMO → LUMO (100)	$\pi_{I2PhOH} \rightarrow \sigma^*_{Pd-Cl} + \sigma^*_{Pd-N} + \sigma^*_{Pd-O}$	^{1}LMCT/^{1}LLCT/^{1}LC
	S_{30}	5.2333	236.91	0.2389	HOMO-13 → LUMO (47) HOMO-12 → LUMO (17)	$d_{\pi}(Pd) + \pi_{Cl} \rightarrow \sigma^*_{Pd-Cl} + \sigma^*_{Pd-N} + \sigma^*_{Pd-O}$ $d_{\pi}(Pd) + \pi_{Cl} + \pi_{py} + \pi_{I2PhOH} \rightarrow \sigma^*_{Pd-Cl} + \sigma^*_{Pd-N} + \sigma^*_{Pd-O}$	^{1}MLCT/^{1}LLCT/^{1}LC

[a] Vertical excitation energies (E), dominant monoexcitations with contributions (within parentheses) of >15%, the nature of the electronic transition, and the description of the excited state are summarized.

Table S8 DFT calculated composition of the frontier molecular orbitals.

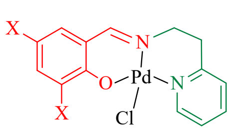

Py-(CH$_2$)$_2$
SalX$_2$

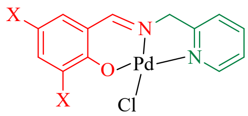

Py-CH$_2$
SalX$_2$

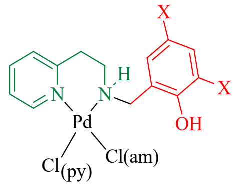

Py-NH
CH$_2$-Ph-OH

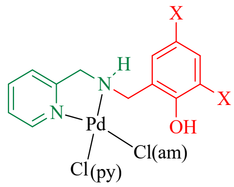

Py-NH
CH$_2$-Ph-OH

	H-4	H-3	H-2	H-1	H	L	L+1	L+2	L+3	L+4
	ClBrPyPd									
Pd	15,83	24,98	65,26	30,36	9,76	47,15	2,83	3,08	1,87	0,99
Cl	32,19	63,29	18,74	31,13	1,91	11,04	0,21	0,49	0,51	0,05
Py-(CH$_2$)$_2$	3,44	7,81	2,93	2,05	2,00	14,65	5,44	95,55	95,68	0,71
SalX$_2$	48,54	3,92	13,08	36,46	86,32	27,16	91,52	0,88	1,94	98,25
	I$_2$PicPd									
Pd	62,66	14,11	33,47	24,94	9,22	46,44	3,43	2,62	0,20	0,45
Cl	29,02	35,25	30,69	20,70	2,02	10,53	0,11	0,04	0,01	0,06
Py-CH$_2$	3,73	0,39	1,87	2,86	1,55	15,33	7,58	95,55	0,17	97,45
SalX$_2$	4,60	50,25	33,97	51,50	87,21	27,69	88,88	1,79	99,61	2,04
	Cl$_2$Py(R)Pd									
Pd	51,98	19,16	73,07	50,21	0,40	46,11	3,57	2,60	2,25	0,40
Cl(py)	3,98	69,59	13,58	40,85	0,25	12,00	0,47	0,02	0,43	0,04
Cl(am)	35,38	2,87	5,30	2,62	0,26	11,42	0,14	0,89	0,21	0,13
Py-NH	6,74	8,00	6,68	2,98	0,90	28,10	95,34	9,32	96,20	5,55
CH$_2$-Ph-OH	1,92	0,38	1,37	3,35	98,19	2,37	0,48	87,16	0,90	93,89
	Br$_2$Py(R)Pd									
Pd	4,33	19,24	74,50	48,07	0,33	46,06	3,59	2,64	2,28	0,29
Cl(py)	9,94	64,62	11,37	40,84	0,18	12,05	0,44	0,02	0,44	0,03
Cl(am)	2,73	2,70	5,00	3,08	0,24	11,42	0,15	0,92	0,19	0,03
Py-NH	3,96	7,71	6,75	2,94	0,72	28,06	95,36	8,83	96,35	0,43
CH$_2$-Ph-OH	79,05	5,72	2,37	5,07	98,53	2,41	0,45	87,59	0,74	99,22
	I$_2$Py(R)Pd									
Pd	19,82	65,01	52,68	11,21	0,29	46,02	3,58	0,10	2,25	2,81
Cl(py)	68,48	20,00	27,86	11,33	0,15	12,03	0,47	0,02	0,45	0,02
Cl(am)	3,42	5,91	1,99	1,44	0,21	11,47	0,15	0,02	0,15	0,97
Py-NH	8,11	5,90	3,56	2,81	0,68	27,99	95,35	0,22	96,32	9,66
CH$_2$-Ph-OH	0,17	3,18	13,91	73,21	98,66	2,49	0,45	99,64	0,82	86,55
	ClBrPy(R)Pd									
Pd	4,61	19,61	73,71	48,79	0,36	46,09	3,57	2,60	2,27	0,42
Cl(py)	8,49	65,67	12,27	39,90	0,21	12,05	0,45	0,02	0,44	0,04
Cl(am)	3,16	2,84	5,00	2,90	0,25	11,41	0,14	0,90	0,21	0,14
Py-NH	4,17	7,85	6,56	3,15	0,79	28,08	95,35	9,16	96,24	5,77
CH$_2$-Ph-OH	79,57	4,03	2,45	5,25	98,39	2,37	0,48	87,32	0,85	93,63
	Br$_2$Pic(R)Pd									
Pd	51,58	63,41	29,27	40,02	0,34	46,41	3,75	0,85	0,77	0,19
Cl(py)	10,94	7,19	4,26	45,45	0,16	12,93	0,15	0,07	0,13	0,02
Cl(am)	29,32	4,54	2,65	9,88	0,65	11,43	0,22	0,25	0,15	0,06
Py-NH	7,43	3,56	6,93	1,90	0,57	26,59	94,82	48,57	54,47	0,37

CH_2-Ph-OH	0,74	21,30	56,88	2,74	98,28	2,65	1,06	50,26	44,48	99,35
	I_2Pic(R)Pd									
Pd	47,41	83,33	39,09	2,98	0,33	46,46	3,73	0,04	0,84	0,87
Cl(py)	20,06	2,77	47,97	0,68	0,13	12,90	0,15	0,00	0,12	0,07
Cl(am)	24,72	4,30	11,42	0,37	0,59	11,45	0,23	0,01	0,15	0,26
Py-NH	6,62	6,89	1,10	3,62	0,55	26,63	94,94	0,13	75,68	27,51
CH_2-Ph-OH	1,20	2,72	0,42	92,36	98,40	2,56	0,96	99,81	23,22	71,28

Table S9 DFT calculated chemical descriptors.

	E(HOMO)	E(LUMO)	I.P.	E.A.	Gap(H-L)	η	σ	μ	ω
Cl_2Pic(R)	-5,873	-0,726	5,873	0,726	-5,147	5,147	0,194	-3,300	1,058
Cl_2Pic	-6,087	-1,614	6,087	1,614	-4,473	4,473	0,224	-3,851	1,657
Cl_2Py(R)Pd	-6,195	-2,477	6,195	2,477	-3,718	3,718	0,269	-4,336	2,528
ClBrPy(R)Pd	-6,157	-2,475	6,157	2,475	-3,682	3,682	0,272	-4,316	2,530
ClBrPicPd	-5,693	-2,044	5,693	2,044	-3,649	3,649	0,274	-3,869	2,051
Br_2Py(R)Pd	-6,118	-2,472	6,118	2,472	-3,646	3,646	0,274	-4,295	2,530
I_2PicPd	-5,645	-2,025	5,645	2,025	-3,620	3,620	0,276	-3,835	2,031
Br_2Pic(R)Pd	-6,188	-2,587	6,188	2,587	-3,601	3,601	0,278	-4,388	2,673
Cl_2PyPd	-5,671	-2,088	5,671	2,088	-3,583	3,583	0,279	-3,880	2,100
I_2Py(R)Pd	-6,029	-2,462	6,029	2,462	-3,567	3,567	0,280	-4,246	2,527
ClBrPyPd	-5,637	-2,081	5,637	2,081	-3,556	3,556	0,281	-3,859	2,094
Br_2PyPd	-5,615	-2,072	5,615	2,072	-3,543	3,543	0,282	-3,844	2,085
I_2Pic(R)Pd	-6,076	-2,581	6,076	2,581	-3,495	3,495	0,286	-4,329	2,680

Hardness (η); Softness (σ); Electronic. Chemical Potential (μ); Electrophilicity Index (ω)

Table S10 Cytotoxicity and chemical hardness of palladium complexes.

	Cell viability % (±SD)	η
ClBrPicPd	10 ± 4	3.649
I_2PicPd	100 ± 2	3.620
Br_2Pic(R)Pd	4.9 ± 1.1	3.601
I_2Pic(R)Pd	6.5 ± 2.5	3.495
Cl_2PyPd	5.4 ± 1.3	3.583
Br_2PyPd	6.7 ± 4.5	3.543
ClBrPyPd	6.7 ± 2.2	3.556
Cl_2Py(R)Pd	79 ± 5	3.718
ClBrPy(R)Pd	47 ± 11	3.682
Br_2Py(R)Pd	61 ± 2	3.646
I_2Py(R)Pd	61 ± 3	3.567